Author	Mohamed Ibrahim Selmy Ahmed
Title	Design of Memristor Device Based Voltage Controlled Oscillator Circuits
Faculty	Engineering
Department	Electrical Engineering
Section	Electronics and Communications
Location	Port Said
Degree	Master of Science
Date	2020
Language	English
Supervision Committee	Assoc. Prof. Ahmed Ahmed Shaaban Dessouki Assoc. Prof. Hassan Mostafa Hassan

English Abstract

The voltage controlled oscillator (VCO) is the oscillator circuit whose output frequency is controlled by a variable dc control voltage. The VCO can be used in many applications such as neural stimulation and heart stimulation. Neural stimulation is one of the most important stimulations in biomedical engineering because it is used to treat the chronic pain such as Parkinson's disease.

In this thesis, the voltage controlled oscillator circuit is represented in two different designs. The first design uses resistors, and the other one uses memristors and both shapes are practically applied. The first one is a voltage controlled oscillator circuit by resistors which uses the fixed resistor and it is designed to work in the low frequency range but the design needs large silicon area to be fabricated which makes its manufacturing cost is high. The second one is proposed a new voltage controlled oscillator using memristors which can be used in low frequency application such as neural stimulation and requires less area and thus less cost. Finally, the thesis provides a comparison between VCO based resistors and memristors for different applications. The comparison helps to recognize the advantages and disadvantages of each type regarding these applications.

Key Words	Memristor – Voltage Controlled Oscillator – Deep Brain Stimulator – Parkinson's disease – Electrical Neural Stimulation.

Acknowledgements

First and foremost, I am grateful to Allah, for all his blessings and for giving me this opportunity to carry on this work, helping, and giving me strength to accomplish it.

I would like to express my great appreciation and deep gratitude to my advisors **Assoc. Prof. Ahmed Shaaban Dessouki** and **Assoc. Prof. Hassan Mostafa Hassan** for their valuable guidance, motivation, precious advice, and constructive comments, their generous, time and effort throughout all the stages of conducting this thesis. Without their help, this work would not have been accomplishment.

Special thanks to **Dr. Sherief Fathi** who provides me with his valuable advice, his extensive discussions, and continuous encouragement. I will never be able to thank him enough for everything I have learned from him.

I would also like to express my sincere gratitude to my professors, colleagues, and friends for their cooperation and continuous support during this work.

Last, but not least, I deeply thank my Family for giving me hope and support. Without their encouragement and constant guidance, I would not have finished this thesis. May Allah bless my great father, and have mercy on my late mother with pardon and forgiveness.

Summary

The voltage controlled oscillator (VCO) is the oscillator circuit whose output frequency is controlled by a variable dc control voltage. The VCO can be used in many applications such as neural stimulation and heart stimulation. Neural stimulation is one of the most important stimulations in biomedical engineering because it is used to treat the chronic pain such as Parkinson's disease.

In this thesis, the voltage controlled oscillator circuit is represented in two different designs. The first design uses resistors and the other one uses memristors and both shapes are practically applied. The first one is a voltage controlled oscillator circuit by resistors which uses the fixed resistor and it is designed to work in the low frequency range but the design needs large silicon area to be fabricated which makes its manufacturing cost is high. The second one is proposed a new voltage controlled oscillator using memristors which can be used in low frequency application such as neural stimulation and requires less area and thus less cost. Finally, the thesis provides a comparison between VCO based resistors and memristors for different applications. The comparison helps to recognize the advantages and disadvantages of each type regarding these applications.

Table of Contents

List of Tables

List of Figures

List of Appendices

Appendix A

Know Data Sheet

Appendix B

Analog Discovery 2 Reference

List of Abbreviations

CMOS	**C**omplementary **M**etal–**O**xide–Semiconductor
VCO	**V**oltage **C**ontrolled **O**scillator
RTDs	**R**esonant **T**unneling **D**iodes
SPICE	**S**imulation **P**rogram with **I**ntegrated **C**ircuit **E**mphasis
ADS	**A**dvanced **D**esign **S**ystem
TiO_2	**T**itanium Di**o**xide
RRAM	**R**esistive **R**andom-Access **M**emory
MIM	**M**etal-**I**nsulator-**M**etal
FPGAs	**F**ield **P**rogrammable **G**ate **A**rrays
MRAM	**M**agnetic **R**andom-**A**ccess **M**emory
VTEAM	**V**oltage **T**hreshold **A**daptive **M**emristor
TEAM	**T**hreshold **A**daptive **M**emristor
GMR	**G**iant **M**agneto **R**esistive
PCM	**P**hase **C**hange **M**emory
CBRAM	**C**onductive **B**ridge **R**andom-**A**ccess **M**emory
Ferbam	**F**erroelectric **R**andom-**A**ccess **M**emory
DC	**D**irect **C**urrent
RFID	**R**adio **F**requency **I**ntegrated **D**evices
DBS	**D**eep **B**rain **S**timulation
PD	**P**arkinson's **D**isease
PI	**P**ostural **I**nstability
STN	**S**ubthalamic **N**ucleus
LFS	**L**ow-**F**requency **S**timulation
HFS	**H**igh-**F**requency **S**timulation
OTAs	**O**perational **T**ransconductance **A**mplifiers
SDC	**S**elf-**D**irected **C**hannel

Cr	**C**hromium
Sn	**T**in
W	**T**ungsten
MSS	**M**ulti-**S**table **S**witch
PCB	**P**rinted **C**ircuit **B**oard

List of Symbols

q	Electric Charge
Φ	Magnetic Flux
M	Emittance
W (*φ*)	Inverse of The Emittance (Mendicancy)
D	The Total TiO_2 Length
w(t)	State Variable
R_{ON}	The Equivalent Resistance of The Memristor
μv	The Average Ion Mobility
R_{OFF}	The Equivalent Resistance of The Memristor
F(w/D)	Window Function
V	Voltage
R	Resistance
C	Capacitance
L	Inductance
F	Frequency
T	The Time Period
V_+	The Positive Voltage of positive node of Opdam
V-	The Negative Voltage of Negative node of Opdam
V_O	Output Voltage
V_{IN}	Input Voltage
V_C	Voltage Control
β	Constant
V_{TL}	The Voltage at Threshold Low
V_{TH}	The Voltage at Threshold High
VDD_+	The Positive Voltage of The Output Signal
VDD_-	The Negative Voltage of The Output Signal

A	Area of Memristor
L	Length of Memristor
Z	Width of Memristor
I	The Total Current
$\mathbf{I_m}$	The Memory-Dependent Current
$\mathbf{I_S}$	Schottky Diode Current

Chapter 1

Introduction

This chapter introduces the statement of the problem. Also, main objectives and the organization of this thesis.

1.1 Introduction and Motivation

CMOS technology was the most important semiconductor integrated circuit technology over the last three decades. However, the minimizing size of CMOS scaling down, which is considered as the important key for continuous progress in the silicon-based semiconductor industry, suffers from increasing technological difficulties. Moreover, the scaling down becomes nearer to the atomic dimension leads to increasing the quantum mechanical tunneling and other non-linear effects on the device performance. For example, in the deep submicron, the power consumption due to the subthreshold and gate leakage currents become a real bottleneck. Thus, many alternative technologies are being investigated to replace CMOS technology or to be integrated with it. Among the emerging technologies, memristor-based technologies are very promising ones.

The memristor is considered as the missing fourth element which is discovered by Leon Chua. The device is a passive two-terminal electrical components that relates the magnetic flux φ with the electric charge q. The memristor is described as inherent nonvolatile property and its dependence on the historic profile of current –voltage. Moreover, the memristor is considered as a strong candidate element for many applications such as Biomedical applications, memristor-based memory, and neuromorphic

circuits. Neuromorphic circuits are the most important ones that greatly benefit from memristive properties.

1.2 Problem Statement

One of the most important circuits used in modern communication systems is the voltage controlled oscillator (VCO). Voltage controlled oscillator is a type of oscillator where the frequency of the output oscillations can be controlled by varying the amplitude of an input voltage signal.

The communication industry evolves, especially in the wireless domain, there will be greater demand for faster data rates, smaller devices, and lower power consumption. These demands will push the development of VCO design beyond today's limitations.

The sustained growth in micro-fabrication technologies over the past two decades led to the development of nanometer-scale semiconductor devices. As the size of a device scales down to that of an electron wavelength, quantum effects take over and new device concepts are needed beyond those used classically.

The most promising of such devices are based on quantum effects. The Resonant Tunneling Diodes (RTDs) and the Memristor. They provide high switching speed operation in the Terahertz regime.

1.3 Thesis Objectives

The main objective of this thesis is to propose quantum devices - based VCO circuits using the Memristor device to achieve the best trade-off among performance, energy, and area. Simulation and design of these circuits will be carried out using computer aided analysis and design tools.

To achieve this main objective, it is broken down into the following specific objectives:

1. Survey on the operation principles of the memristor, its modeling, application, and analysis.
2. Define the main problems of the current Voltage Controlled Oscillator circuits.
3. Study some current techniques to design the Voltage Controlled Oscillator circuits.
4. Propose effective Voltage Controlled Oscillator circuits in terms of the area, the power consumption, and the range of oscillation. These circuits will be based on the memristor.
5. Design and analysis of the proposed circuits by using computer aided design software such as SPICE, Advanced Design System (ADS) software, or Cadence.
6. Analysis, and discuss the simulated results.
7. The proposed circuits are practically applied.
8. Conclusion the thesis and propose recommendations for future works.

1.4 Thesis Organization

The thesis is organized as follows:

Chapter 1 presents the introduction and the scope of the thesis.

Chapter 2 reviews the background of the main aspects of the memristor, VCO and Biomedical. Chapter two provides these aspects which include

how the memristor works. Defines the different types of modeling techniques for memristors, defines how the VCO work and its applications, and discusses some biomedical applications.

Chapter 3 introduces the design of memristor-based VCO for biomedical applications, provides the proposed memristor-based VCO circuit, simulation results, the comparison between the proposed circuit and the reference circuit.

Chapter 4 discusses the experimental setup and testing of the proposed circuit, presents the industrial memristor and simulation result. Provides the experimental results and discussion.

Chapter 5 provides the conclusion and the recommendations for future work. Finally, the list of references and the appendices are provided.

Chapter 2

Background

The current chapter is divided into two sections. The first section reviews the background of the main aspects of the memristor. Moreover, this section presents the history of the memristor and its applications. The second section provides an overview of the Voltage Controlled Oscillator and its applications with a special focus on VCO for biomedical applications.

2.1 Introduction to Memristor

According to circuit theory, before 1971, there are only three fundamental passive circuit elements: resistor, inductor, and capacitor. In 1971, Professor Leon Chua introduced the fourth element, which is memristor. Memristive devices can be defined as devices that have hysteresis zero-crossing current-voltage characteristics [1].

At the same time, the other two proposed devices share the same concept of the memristor denoted by the memcapacitor and the meminductor [2].

The name “memristor” stands for memory-resistor. The memristors acts as the device acts as a resistor with memory and represents the relationship between the electric charge (q) and the magnetic flux (Φ) as shown in Fig.2.1 [1]. The memristor’s parameter is called the memristance (M), and it is measured in ohms. As the current is the time integration of the electric charge and the voltage is the time integration of the magnetic flux. The memristance value changes depending on the historic profile of

the applied voltage on the memristor terminals and the historic profile of the current passed through it. That is why this element is denoted as a memristor; which is short of "memory-resistor".

A team at HP Labs, in 2008, developed the first prototype of the memristor by using two terminal elements that achieve the characterization of the memristor [3]. The HP memristor is a solid-state two terminal devices formed of a nanometer scale titanium dioxide (TiO2) thin film sandwiched between two metal contacts as shown in Fig.2.2. The TiO2 layer is divided into two layers, one layer is an undoped layer and the second one layer is a doped layer [4]. The device achieved the main memristor properties according to Prof. Chua definition.

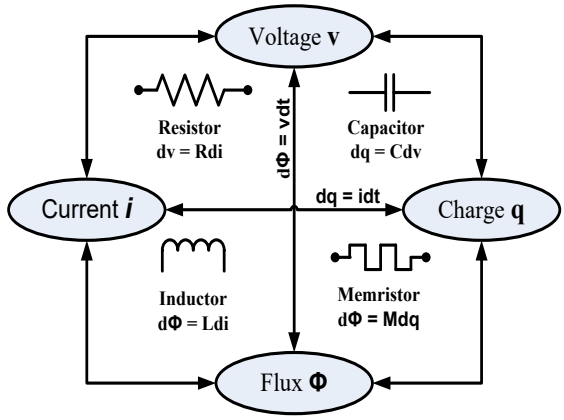

Fig.2.1 Fundamental electrical elements relationships [1].

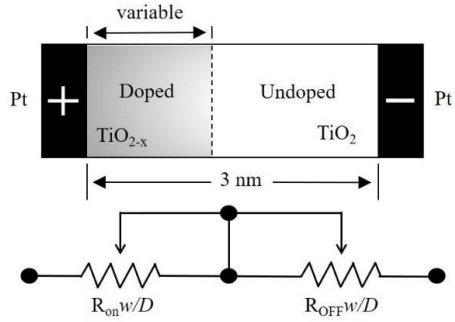

Fig.2.2 HP TiO2 Memristor [3].

2.2 Device Properties

According to Fig.2.1, the memristor represents the relationship between the electric charge (q) and the magnetic flux (Φ) . The q-φ relationship is nonlinear and the memristor parameter is called as memristance (M).

The memristor is described as the charge-controlled memristor when its memristance is dependent on the change of flux with charge, where M (q) equals:

$$M(q) = {}^{d\varphi}/_{dq} \tag{2.1}$$

On the other hand, the memristor is described as the flux-controlled memristor when its memductance (W) is dependent on the change of charge with flux. W (φ) is the inverse of the memristance and it equals:

$$W(\varphi) = {}^{dq}/_{d\varphi} \tag{2.2}$$

For the charge-controlled memristor, the current-voltage relationship is:

$$v = M(q)\,.\,i \tag{2.3}$$

For the flux-controlled memristor, the current-voltage relationship is:

$$i = W(\varphi)\,.\,v \tag{2.4}$$

The device properties can be summarized as follows: Nano-scale device, Bipolar device, Great resiliency, reliability when power is interrupted, Memristance consideration, High data density, Frequency response, and Asymmetry ON/OFF switching behavior [5].

2.2.1 Memristor's Working Principle

The operation of the TiO2 memristor is described as follows: when applying a voltage on the terminals of the memristor, the oxygen vacancies move from one side to the other side. The width of the doped layer (w) decreases or increases based on the polarity of the applied voltage. The memristor is ON when the doped layer increases and OFF when the doped layer decreases. The memristor is special because when no voltage source applied the oxygen vacancies do not move (i.e., keep in the same position). This phenomenon makes the memristor remembers the last applied voltage and use it as non-volatile memory [6]. Fig.2.3 explains the process of the memristor when positive and negative voltages are applied.

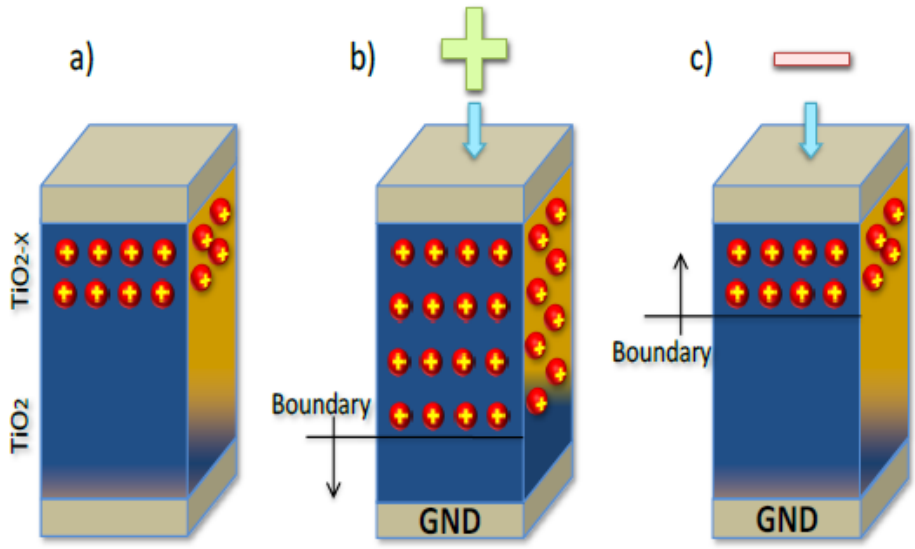

Fig.2.3 (a) memristor structure. (b) when applied positive voltage, oxygen vacancies move toward the undoped region. c) when applied negative voltage, oxygen vacancies move toward the doped region [6].

2.2.2 Current- Voltage (I-V) Characteristic

Fig.2.4. shows the difference between the current-voltage characteristic of the four fundamental elements. As shown in the figure, the memristor has a hysteresis current-voltage characteristic.

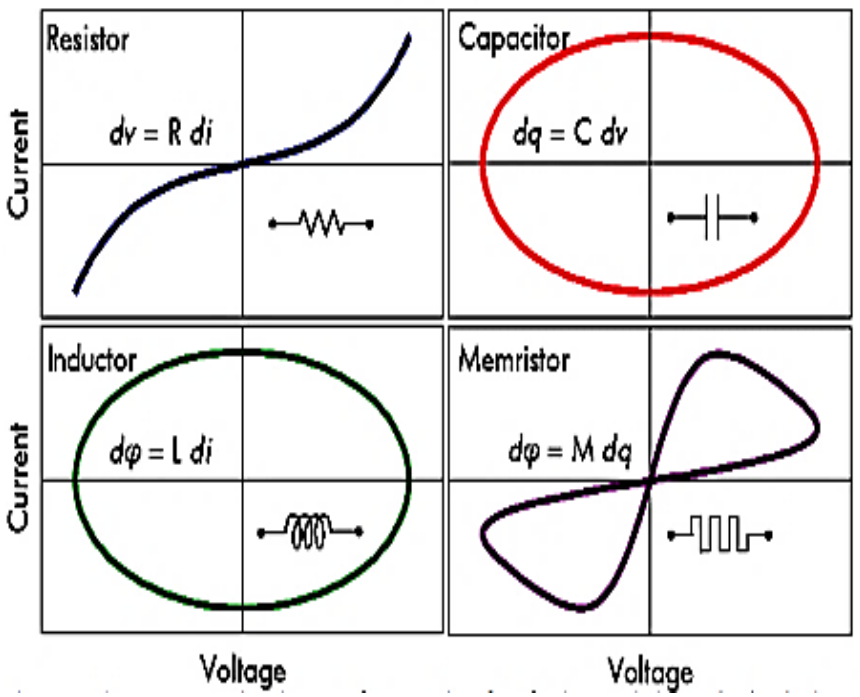

Fig.2.4 Current-voltage characteristics for the resistor, capacitor, inductor and memristor [7].

2.3 Types of Memristors

The memristor can be made different types of materials. So, the memristor used different implementations. The most important types of memristors are the resistive and spintronic memristors.

2.3.1 Resistive Memristors

The resistive memristors are based on thin resistive film sandwiched between two metal electrodes in a way similar as shown in Fig.2.2 [2]. The resistivity of resistive memristor must be changed under the motion of electric current showing the hysteresis current-voltage relationship. This type of memristor is used in the construction of Resistive Random Access Memory (RRAM) cells. Fig.2.5 shows the general design of resistive memristors. It consists of resistive material between two metal electrodes which can be done through the metal-insulator-metal (MIM) technique [8].

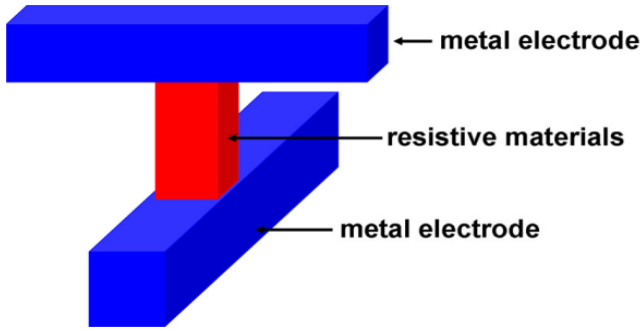

Fig.2.5 Resistive memristor based on MIM architecture [8].

Resistive memristors can be built by using various materials such as TiO2, ZnO, and TaOx [9, 10]. However, these types were built years ago, the physical interpretation of the switching mechanism is still not confirmed.

Titanium dioxide memristor is a solid-state resistive memristor which was physically realized at HP labs in 2008 [3]. The HP memristor's basic structure, as shown in Fig.2.2. It consists of a layer of TiO2 sandwiched

between two Platinum electrodes. The TiO_2 layer is divided into doped and undoped parts. The boundary between the doped and undoped "TiO_2" is called as the “domain-wall”. The domain-wall position (state) changes under the effect of the applied voltage or current.

The titanium dioxide memristor is composed of a thin (50 nm) titanium dioxide film between two 5nm thick electrodes, one is titanium, and the other is platinum. The titanium dioxide film consists of two layers. One of these layer has a slight depletion of oxygen atoms (undoped). The other layer is the doped layer with oxygen vacancies. The doped layer has a much lower resistance than the undoped layer.

2.3.2 Spintronic Memristors

The three different possible designs of spin-transfer torque based magnetic memristors were described in Chen et al. [11]. The important structure in the three different designs is the domain-wall spintronic memristor, in which the device's resistance occurs when the spin of electrons in one section of the device points in a different direction from those in another section. This creates a boundary between the two sections called as “domain wall”. Electrons flowing into the device have a certain spin, which alters the device’s magnetization state. Changing the magnetization of the device moves the domain wall and changes its resistance.

Spintronic memristors are considered important elements for many applications, such as memory chips [12, 13], and neuromorphic circuits [14, 15]. In the field of memory circuits, spintronic memristors are considered as one of the promising candidates for high-performance and

high-density storage technologies because of introducing excellent scalability, and non-volatility properties.

In the field of logic circuits, a new type of implied logic using memristors is presented in [16]. The memristor-based logic has the unique ability to be fabricated with memory cells on the same chip. The memristor is also used in crossbar arrays in switching blocks of field programmable gate arrays (FPGAs) [17, 18].

The spintronic memristor has the potential to be a non-volatile memory element, since it holds its resistive value, even after it is unplugged from a power source. It also has the advantages of Magnetic Random-Access Memory (MRAM) such as radiation hardness, and mature memory technology. Thus, the spintronic memristor-based memory devices would be the future of non-volatile memories.

2.3.3 Other Types of Memristors:

There are other possible Kinds of memristors such as Polymeric Memristor [8, 19], Ferroelectric memristor [8, 20, 21], Manganite memristor [8], and Resonant-tunneling diode memristor [8]. All these types of memristors are well reviewed and explained in [8].

2.4 Review of Existing models for Memristor Simulation

It is important to know how the memristor works with an external stimulus in terms of voltage and current. In this section, I will show the main models of memristors.

2.4.1 Linear Ion Drift Model:

The linear ion drift model depends on the HP memristor, as shown in Fig.2.2. In this model, a uniform electric field across the device is assumed; thus, there is a linear relationship between drift-diffusion velocity and the net electric field. So, the state equation that describes the relationship can be written as follows [3]:

$$\frac{dw(t)}{dt} = \mu_V \frac{R_{ON}}{D} i(t) \tag{2.5}$$

Where D is the total TiO_2 length, w(t) is a state variable defining the length of the doped TiO_2, R_{ON} is the equivalent resistance of the memristor when the whole device is doped and μ_V is the average ion mobility.

According to the linear ion drift, the memristor can be modeled as a coupled variable-resistor model as shown in Fig.2.6, yielding the following I-V relationship [3]:

$$\mathrm{v}(t) = \left(R_{ON}\frac{w(t)}{D} + R_{OFF}\left(1 - \frac{w(t)}{D}\right)\right) i(t) \tag{2.6}$$

where R_{OFF} is the equivalent resistance of the memristor when the whole device is undoped.

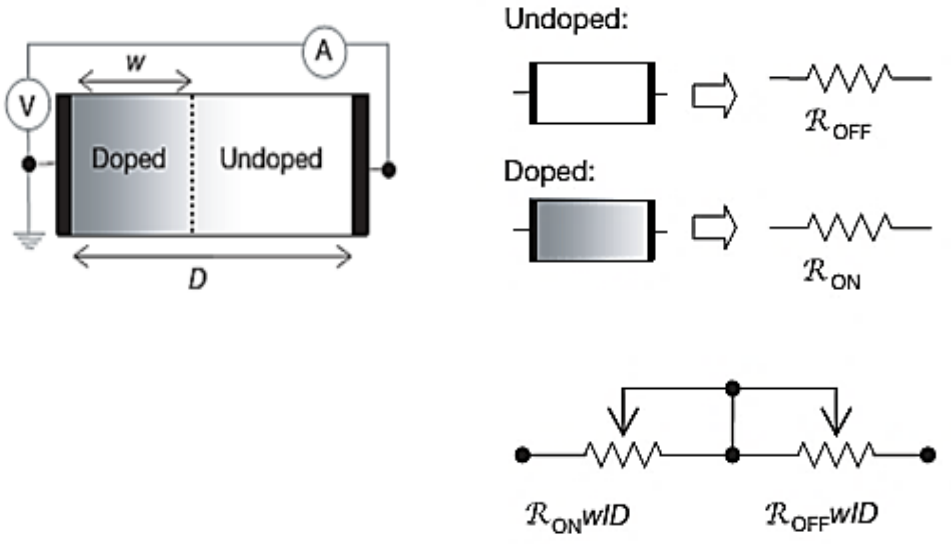

(a) **(b)**

Fig.2.6 The coupled variable-resistor model for a memristor (a) Memristor Device (b) Equivalent resistor model [3].

Solving Eqs. (2.5) and (2.6), the memristance of the device, for $R_{OFF} >> R_{ON}$ can be simplified to:

$$M(q) = R_{OFF}\left(1 - \frac{\mu_V R_{ON}}{D^2} q(t)\right) \tag{2.7}$$

The coupled equations of motion for the charged dopants and the electrons in this device take the normal form for a current-controlled (or charge-controlled) memristor as in Eqs. (2.5) and (2.6).

2.4.2 Nonlinear-Ion Drift Model:

Applying a few volts on the nanometer dimensions of memristor can cause a high electric field. Thus, the electric field can easily exceed 10^6

V/cm, and cause a high nonlinearity. The linear drift assumption also suffers from a problem in incorporating boundary effects.

The state equation can be modified by using a window function *F(w/D)*. The window function is multiplied by the right-hand side of Eq (2.5) and the new state equation becomes as follows:

$$\frac{dw(t)}{dt} = \mu_V \frac{R_{ON}}{D} i(t) F\left(\frac{w}{D}\right) \quad (2.8)$$

The window function should satisfy F (0) = F (1) =0 to ensure no drift at the boundaries because the speed of the boundary (v_d) that is founded between the doped and undoped regions needs to be strongly suppressed when it approaches either edges, w~0 or w~D.

Many papers proposed different window functions such as the window function that was proposed by Joglekar [22] and the one that was proposed by Biolek [23].

2.4.3 Simmons's Tunnel Barrier Model:

The Simmons tunnel barrier model for simulating TiO_2 memristive devices was proposed by Pickett et al. [24] who are members of the HP lab team.

The theory of this model and the window function are explained in [24]. This model assumes nonlinear and asymmetric switching behavior of the TiO2 memristor.

2.4.4 TEAM Model:

The TEAM model is provided in [25] which is considered as a simple model. This model compromises the simplicity of the linear ion-drift model and the accuracy of the Simmons tunnel barrier model.

2.4.5 VTEAM Model:

The VTEAM model is provided in [26]. The VTEAM model and the TEAM model are very similar. The VTEAM introduces the voltage threshold and the TEAM model introduces the current threshold.

2.4.6 Verilog-A Models:

The Verilog-A code for the TEAM model is available in [27].

2.4.7 Spintronic Memristors Modeling:

The spintronic memristor can be modeled by using any empirical memristor model. There are only two available models.

The first model is proposed by Chen et al. [28] for a CIP giant magnetoresistive (GMR)-based spintronic memristor. The second model is a CPP GMR-based spintronic memristor model proposed by Miao Hu et al. [29].

2.5 Memristor Applications:

Memristors have unique properties that make them novel devices with new capabilities that permit great opportunities in different applications, for example; memory chips, neuromorphic systems, logic circuits, FPGA switching blocks, neural and neuro-fuzzy networks programmable logic and processing configurations, chaotic circuits, and others [30].

In the field of memory chips, the memristor is a very promising device because it can remember its previous state. The main features that are required for next-generation memory chips are high-performance and high density. The inherent non-volatility and excellent scalability of memristors can help in the design of memory circuits. Memristors can be used in cell structures of memories such as Resistive Random Access Memory (RRAM) cell structures.

The memristor applications for analog, digital, and chaos applications have been discussed in [31]. The memristor digital applications include Threshold comparators, Schmitt triggers, Flip Flops and Multi-state pipeline registers. Also, the memristor analog applications include Chaos circuits, Biometric circuits, and Filters.

The memristor applications for logic applications and the field programmable gate arrays (FPGAs) have been reported in [32].

Neuromorphic circuits are considered the most important applications and are used to emulate the human brain. The nanotechnology underwent a rapid development. So, it provided neuromorphic computing architecture with novel memristive devices which have the capability of mimicking synaptic plasticity, such as resistive switching memory (RRAM), phase change memory (PCM), conductive bridge memory (CBRAM), and ferroelectric memory (FeRAM). The advantages of using these memristive nanodevices to model the behavior of synapses are their unique properties, such as nano size, scalability, and flexibility. These properties are used because of their analog behavior, manufacturability on top of CMOS technology to make a crossbar array and ability to remember the last state [33].

Oscillators are electronic circuits that are used in electronic applications such as timing circuits, modulation, test, and measurement devices. They are divided into sinusoidal or relaxation oscillators. Oscillators are based on reactive elements such as capacitors and inductors to achieve oscillation [34].

The memristor is used to describe the charging and discharging of the reactive elements, where the memristance can be increased or decreased. Therefore, the memristor is considered as a resistance-storing element. In the relaxation oscillators, we can replace a capacitor or inductor by a memristor. The concept of voltage controlled memristor-based relaxation oscillator with a memristor was discussed [34].

2.6 Voltage Controlled Oscillator

2.6.1 What is the Voltage Controlled Oscillator

A voltage-controlled oscillator (VCO) has become a very important building block. Therefore, it is considered as an important element of electronic systems in which output frequency is linearly varied by the input control voltage. The oscillation frequency varies from few hertz to hundreds of GHz. By varying the input DC voltage.

2.6.2 Working Principle of VCO

The voltage controlled oscillator is implemented using different components like transistors, varactor diodes, Op-amps, and etc.

Voltage Controlled Oscillator comes in different forms such as RC oscillator, multivibrator oscillator, LC oscillator, and crystal oscillator type

[35]. In the case of RC oscillator, the oscillation frequency of the output signal is as follows:

$$f = \frac{1}{(2\pi RC)} \tag{2.9}$$

In the case of LC oscillator, the oscillation frequency of the output signal is as follows:

$$f = \frac{1}{(2\pi\sqrt{LC})} \tag{2.10}$$

The working principle of the voltage controlled oscillator is that when the control voltage decreases from a nominal voltage, the frequency also decreases and as the nominal control voltage increases, the frequency also gets higher. When the nominal control voltage that is represented by V_C(nom) is applied, the oscillator works at its free-running or normal frequency, and the nominal frequency is represented by f_C(nom) as shown in Fig.2.7 [35].

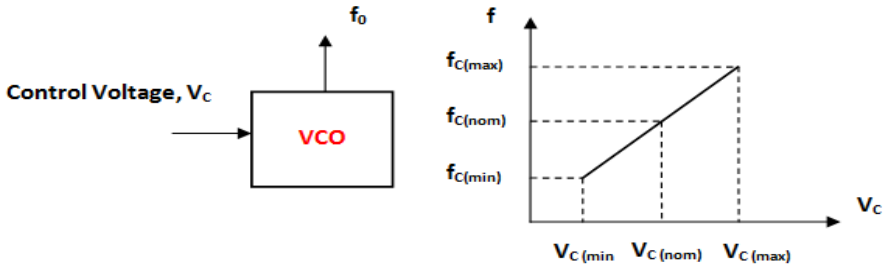

Fig.2.7 The basic working of voltage controlled oscillator [35].

2.6.3Types of Voltage Controlled Oscillators

The voltage-controlled oscillator produces a waveform that can be categorized into two groups namely harmonic oscillators and relaxation oscillators [36].

Harmonic Oscillator:

Harmonic or linear voltage controlled oscillator produces the sinusoidal output waveform. Examples of this type of oscillators are Crystal and LC oscillators [36].

Relaxation Oscillator

These VCOs are used to generate a triangle or sawtooth waveforms. The most common use of VCO is applied into two forms namely VCO as a stable multivibrator and VCO as a Schmitt trigger [36].

2.6.4 Applications of VCO

The major applications of VCOs are optical transmission, clock generation, radio frequency integrated devices (RFID) transponders, data recovery circuits, Phase Locked Loop and also in medical domains such as Biomedical applications [37].

2.7 Biomedical Applications

Physiological Signals hold information that can be extracted from these signals to find out the state of the functioning of these physiological systems and its useful in the prevention, diagnosis, and treatment of diseases [38].

Nowadays, nanotechnology is revolutionizing the approaches in different fields from manufacture to health. With the fast development of the electronic industry, the need for integrated electronics is very important because it's useful for monitoring physiological signals as medical advancement grows into personalized health-care [38, 39].

The design of integrated electronics for biomedical applications helps advance medical research and the development of closed-loop solutions such as brain-machine interfaces for prosthetics control [38].

Biomedical integrated electronics that are embedded in the human body. they are typically limited by the power that can be delivered to the implant. The limited power available to implantable biomedical electronics sets the low power requirement in the design of internal sub-systems [38]. Many nervous system disease treatments need electrical nerve stimulation to repair the damage, for example; the deep brain stimulators.

2.7.1 Biomedical Frequency:

Deep brain stimulation (DBS) is a neurosurgical procedure to stimulate a specific brain area with electric pulses for treatment purposes. It is an important and useful treatment to alleviate various symptoms of neurologic and psychiatric disorders, such as Parkinson's disease (PD), epilepsy and major depression [40].

Parkinson's disease (PD) is a progressive neurodegenerative condition which is characterized by bradykinesia, tremor, rigidity, postural instability (PI), and numerous nonmotor manifestations. Now, many pharmacological therapies exist to successfully treat PD motor symptoms. However, the disease progresses often becomes challenging to be treat with medications alone. Deep brain stimulation (DBS) has become a crucial player in PD treatment, particularly for patients who have disabling motor complications from medical treatment [41].

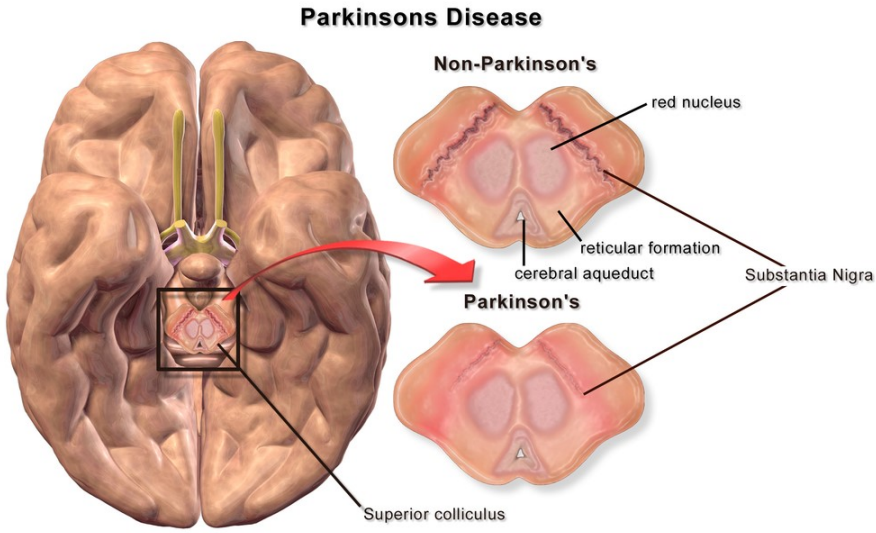

Fig. 2.7 A brain without and with Parkinson's Disease [42].

This study aims to investigate how the frequency settings of deep brain stimulation (DBS) targeting the subthalamic nucleus (STN) influence the motor symptoms of Parkinson's disease (PD). Stimulation with frequencies less than 100 Hz (mostly 60 or 80 Hz) is considered low-frequency stimulation (LFS) and with frequencies greater than 100 Hz (mostly 130 or 150 Hz) is considered as a high-frequency stimulation (HFS) [43].

The frequency of DBS is often categorized as a high frequency (i.e., HFS>100Hz, mostly 130 or 150Hz) or a low frequency (i.e., LFS <100Hz, mostly 60 or 80Hz). These two categories have varied therapeutic effects on motor function in those with PD [43].

The frequency needed to be relieved from Parkinson's disease is different from person to person but it is still in the range from 130 Hz to 185 Hz.

Chapter 3

Design of Memristor – Based Voltage Controlled Oscillator for Biomedical Application

3.1 Introduction

As mentioned in the previous chapter, neural stimulation is one of the most important stimulations in biomedical engineering because it is used to treat chronic pain such as Parkinson's disease. The main challenge in designing a very low frequency oscillator is the large physical dimensions of the passive elements which are used in the circuit. They occupy a large silicon area. Therefore, the memristor can be used instead of the resistor to decrease the silicon area and to achieve low power consumption. The memristor can be utilized in the voltage-controlled oscillator design for electrical neural stimulation because of two important advantages: (1) nanoscale dimensions and (2) low power consumption.

This chapter presents a memristor based new voltage-controlled oscillator for electrical neural stimulation. The proposed circuit generates low frequency range from 104 Hz to 203 Hz with a low power consumption equal 0.79 mW which is the main challenge in deep brain stimulators and the total silicon area is 0.67 mm^2.

3.2 Biomedical Applications

Parkinson's disease (PD) is an inveterate and progressive movement disorder. This means that symptoms keep and worsen as time progresses. Deep brain stimulation in the subthalamic kernel is a therapy that helps the patients to relieve Parkinson’s disease [44]. The frequency needed to be relieved from Parkinson’s disease when it is different from person to person but it is still in the range from 130 Hz to 185 Hz [44].

As mentioned in the previous chapter, the memristor can be used instead of resistance to decrease the silicon area and to achieve low power consumption. The memristor is considered as a nanoscale device so it's useful for many applications such as nonvolatile memory applications, low power, remote sensing applications, crossbar latches as transistor replacement, analog computation and circuit application.

3.3 Previous Work:

As shown in Fig.3.1, a low frequency oscillator proposed using a capacitance converter circuit with an active transconductance element, gm [45]. Such an approach needs small values of gm that is produced by using low-power operational transconductance amplifiers (OTAs). The circuit achieves a frequency range from 0.2 Hz to 5 Hz which is not suitable for the electrical neural stimulation and it makes its operation limited.

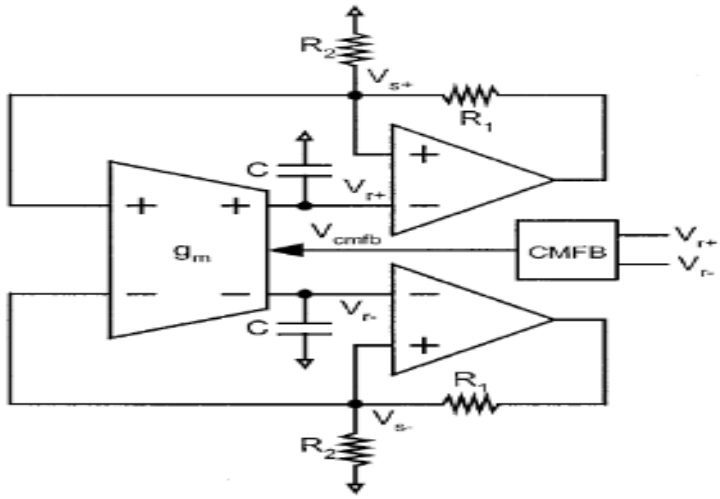

Fig. 3.1 Relaxation Oscillator [45]

In [46], The proposed oscillator, uses the concept of a constant current source and sinks for oscillation as shown in Fig.3.2. The transistor operates in the subthreshold region which is used to reduce the size of the capacitance, in addition to decreasing power dissipation. The circuit achieves a frequency range from 0.3 Hz to 100 Hz and it has better performance in the electrical neural stimulation than which is in [9].

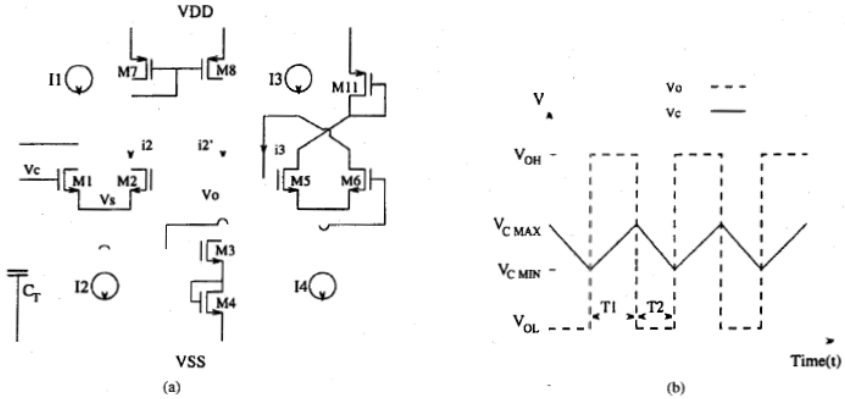

Fig. 1. (a) Very low frequency, micropower, low voltage CMOS oscillator. (b) Wave forms of output V_O and oscillation control voltage V_C.

Fig. 3.2 The proposed oscillator [46].

As shown in Fig.3.3 in [47], a microwave circuit is used to design an LC oscillator to avoid the large size of the capacitor by generating high frequency, using frequency division and mixing circuits to produce low frequency. However, the resultant circuit achieves high power consumption.

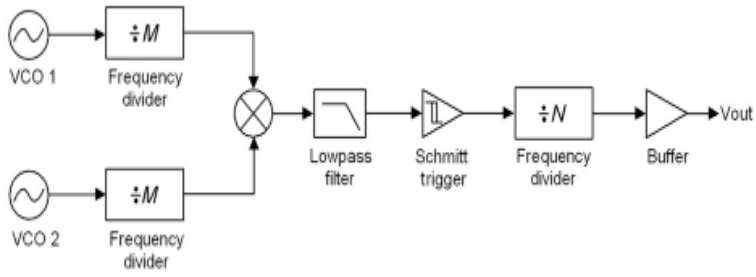

Fig. 3.3 System architecture of the very low – frequency signal generator [47].

3.4 Voltage Controlled Oscillator Specifications

In general, the frequency range that is needed for Parkinson's disease (PD) is from 130 Hz to 185 Hz. So, we need to design a voltage controlled oscillator (VCO) that covers this range.

The main challenge that faces the designing and implementation of a low frequency voltage controlled oscillator (VCO) is how to achieve a wide tuning range with a practical small area and low power constraints to be used in many different applications such as biomedical applications (i.e., in the deep brain stimulation range from 130 Hz to 185 Hz). Generally, the output frequency is inversely proportional to the product of capacitance and resistance as follows:

$$F\alpha\ 1/RC \qquad (3.1)$$

Therefore, the low frequency oscillator needs large values of resistance and capacitance which occupies a large Silicon area. Thus, the memristor can be used instead of a resistor to decrease the silicon area as well as the power consumption.

The next section will show a memristor-based new voltage-controlled oscillator for electrical neural stimulation.

3.4 Proposed Circuit Design

Fig.3.3 shows the system diagram of the proposed low frequency memristor based VCO circuit. It consists of three building blocks; the first block is the voltage controlled oscillator which generates its output frequency in the (KHz) range. The VCO consists of a Schmitt trigger circuit, two operational amplifier stages, and an integrator. The second block is a level shifter circuit that consists of an inverter to change the output VCO voltage rails from (+ V_{DD}, - V_{DD}) to (0, V_{DD}). The third block is a frequency divider which consists of 7 stages D flip-flops to divide the output VCO frequency (i.e., kHz range) to the deep brain stimulation required very low frequency (i.e., Hz range).

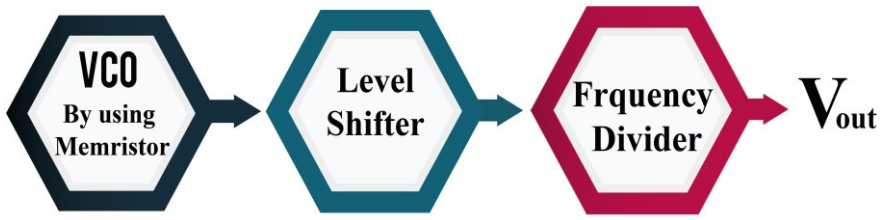

Fig. 3.4 The proposed low frequency deep brain stimulation circuit.

3.4.1 Voltage Controlled Oscillator:

The voltage-controlled oscillator consists of a Schmitt trigger, two-stage operational amplifier and an integrator where the resistors are replaced by memristors as shown in Fig.3.5. The function of the two operational amplifier stages is to introduce fine control of the output signal shape to be pure square pulse by introducing the required delay and gaining along the feedback loop.

The VCO block's output frequency (F) is given by:

$$F = 1/T \tag{3.2}$$

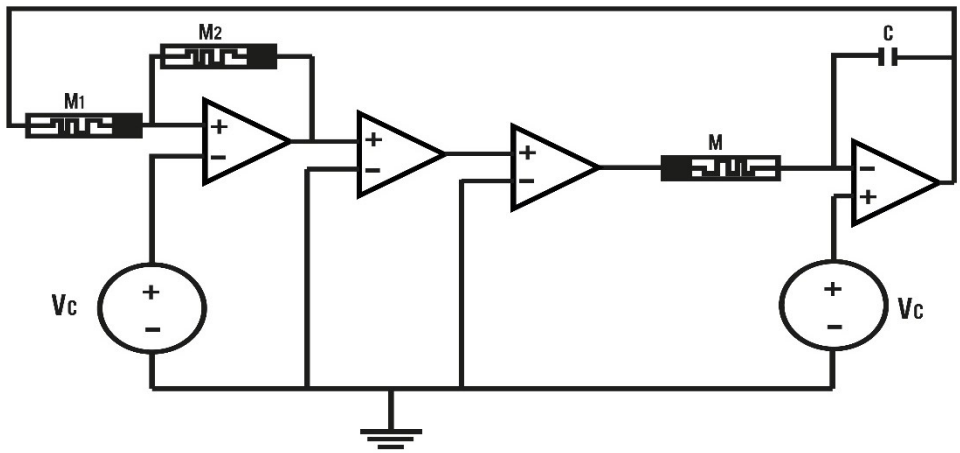

Fig. 3.5 Voltage controlled oscillator building block.

The mathematical model for the time period T is provided by Equations (3.3) to (3.36) as follows:

1- Schmitt trigger:

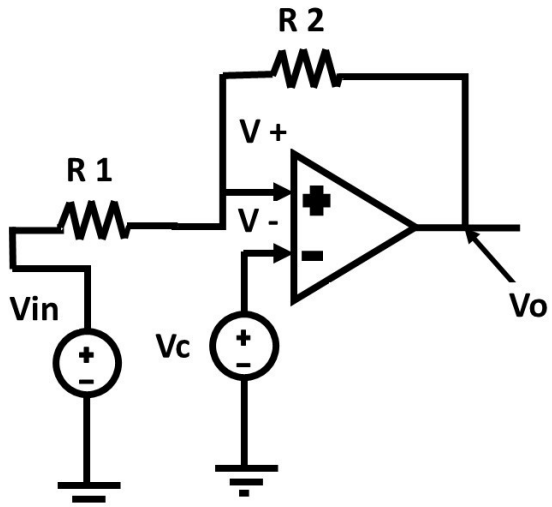

$$v_+ = v_- \tag{3.3}$$

$$v_C - v_- = 0 \tag{3.4}$$

$$v_C = v_- \tag{3.5}$$

$$v_+ = v_{in}\left(\frac{R_2}{R_1+R_2}\right) + v_o\left(\frac{R_1}{R_1+R_2}\right) \tag{3.6}$$

If $v_+ = v_- = v_C$ & $v_{in} = v_{TL}$ & $v_o = L_+$

$$v_C = v_{TL}\left(\frac{R_2}{R_1+R_2}\right) + L_+\left(\frac{R_1}{R_1+R_2}\right) \tag{3.6}$$

$$v_C * (R_1 + R_2) = v_{TL} * (R_2) + L_+ * (R_1) \tag{3.7}$$

$$v_{TL} = \frac{\left(v_C*(R_1+R_2) - L_+*(R_1)\right)}{R_2} \tag{3.8}$$

If $v_+ = v_- = v_C$ & $v_{in} = v_{TH}$ & $v_o = L_-$

$$v_C = v_{TH}\left(\frac{R_2}{R_1+R_2}\right) + L_-\left(\frac{R_1}{R_1+R_2}\right) \tag{3.9}$$

$$v_C * (R_1 + R_2) = v_{TH} * (R_2) + L_- * (R_1) \quad (3.10)$$

$$v_{TH} = \frac{(v_C*(R_1+R_2)-L_-*(R_1))}{R_2} \quad (3.11)$$

2- Integrator

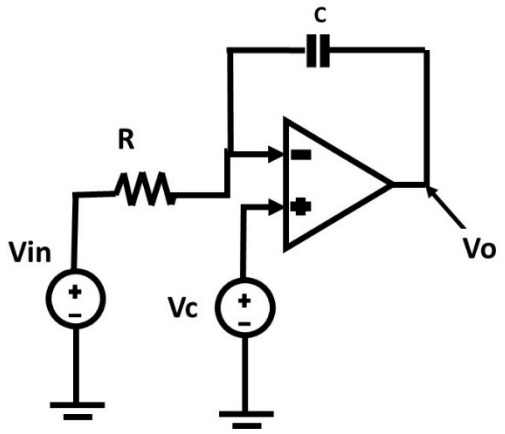

$$\frac{(v_{in} - v_-)}{R} = \mathrm{c} * \frac{(\mathrm{d}(v_- - v_\mathrm{o}))}{\mathrm{dt}} \quad (3.12)$$

$$v_+ = v_- = v_C \quad (3.13)$$

$$\frac{(v_{in} - v_\mathrm{c})}{R} = \mathrm{c} * \frac{(\mathrm{d}(v_\mathrm{c} - v_\mathrm{o}))}{\mathrm{dt}} \quad (3.14)$$

$$\frac{(v_{in} - v_\mathrm{c})}{R*c} = - \frac{(\mathrm{d}(\ v_\mathrm{o}))}{\mathrm{dt}} \quad (3.15)$$

$$\mathrm{d}(\ v_\mathrm{o}) = \ -\frac{1}{R*c} * (v_{in} \ - \ v_\mathrm{c}) * \mathrm{dt} \quad (3.16)$$

If $v_{in} = L_+$

$$v_o(t) = \ -\frac{1}{R*c}\int_0^{t_1}((L_+) \ - Vc)dt \quad (3.17)$$

$$\Delta v = -\frac{((L_+) - Vc)}{R*c}\Delta t \quad (3.18)$$

$$(v_{LH} - v_{TH}) = -\frac{((L_+) - Vc)}{R*c} * (t - 0) \quad (3.19)$$

$$(v_{LH} - v_{TH}) = -\frac{((L+) - Vc)}{R*c} * (t_1) \quad (3.20)$$

$$t_1 = -(v_{LH} - v_{TH}) * (R * c)/((L_+) - Vc) \quad (3.21)$$

If $v_{in} = L_-$

$$v_o(t) = -\frac{1}{R*c}\int_0^{t_2}((L_-) - Vc)dt \quad (3.22)$$

$$\Delta v = -\frac{((L-) - Vc)}{R*c}\Delta t \quad (3.23)$$

$$(v_{LH} - v_{TH}) = -\frac{((L_-) - Vc)}{R*c} * (t_2 - 0) \quad (3.24)$$

$$(v_{LH} - v_{TH}) = -\frac{((L_-) - Vc)}{R*c} * (t_2) \quad (3.25)$$

$$t_2 = -(v_{LH} - v_{TH}) * (R * c) / \big((L_-) - Vc\big) \quad (3.26)$$

$$T = t_1 + t_2 \quad (3.27)$$

$$T = -(R * c)[\left(\frac{R_1}{R_2}\right) * ((L_-) - (L_+)/\big((L_+) - Vc\big) + \left(\frac{R_1}{R_2}\right) * ((L_+) - (L_-)/\big((L_-) - Vc\big)] \quad (3.28)$$

where β is a constant and equals:

$$\beta = \left(\frac{R_1}{R_2}\right) \quad (3.29)$$

$$T = -(R * c) * \beta * ((L_+) - (L_-)[\,(-1)/\big((L_+) - Vc\big) + (1)/\big((L_-) - Vc\big)] \quad (3.29)$$

If $L_+ = -L_-$

$$T = -(R * c) * \beta * 2 * (L_+)[\,(-1)/\big((L_+) - Vc\big) + \,(1)/\big((L_-) - Vc\big)] \quad (3.30)$$

$$T = -(R * c) * \beta * 2 * (L_+)[\,(L_+) + Vc + (L_+) - Vc/\big((L_+) - Vc\big) * \big((-L_+) - Vc\big)] \quad (3.31)$$

$$T = -(R * c) * \beta * 2 * (L_+)[\,(L_+) + (L_+)/\big((L_+) - Vc\big) * \big((-L_+) - Vc\big)] \quad (3.32)$$

$$T = -(R * c) * \beta * 2 * (L_+)[\,2 * (L_+)/\big((L_+) - Vc\big) * \big((-L_+) - Vc\big)] \quad (3.33)$$

$$T = -(R * c) * \beta * 2 * (L_+)[\,2 * (L_+)/\big((L_+) - Vc\big) * -\big((L_+) + Vc\big)] \quad (3.34)$$

$$T = \,(R * c) * \beta * 4 * (\,L_+^2)[\,1/\big((L_+) - Vc\big) * \big((L_+) + Vc\big)] \quad (3.35)$$

The final form of the time period T is given by:

$$T = \,4 * R * c * \beta * (\,L_+^2)[\frac{1}{\big((L_+^2) - V_c^2\big)}] \quad (3.36)$$

The voltage-controlled oscillator replaced the resistors by memristors as shown in Fig.3.5. The final detection after replacing resistance (R) by memristance (M) will be:

$$T = \,4 * M * c * \beta * (\,L_+^2)[\frac{1}{\big((L_+^2) - V_c^2\big)}] \quad (3.37)$$

where M is the integrator input memristance value that is designed such that M equals R_{OFF}, C is the capacitance value. β is the value of $(M1/M2\,)$ where M1 and M2 are Schmitt trigger circuit input memristance

and feedback memristance values; L_+ is the value of VDD_+ of circuit and Vc is the control voltage value that varies from 0.1 V to 0.7 V.

3.4.2 Level Shifter:

The level shifter is achieved by using an inverter, as shown in Fig3.6, to shift the output frequency limits which are generated by the VCO; from (+ VDD, - VDD) to (0, + VDD).

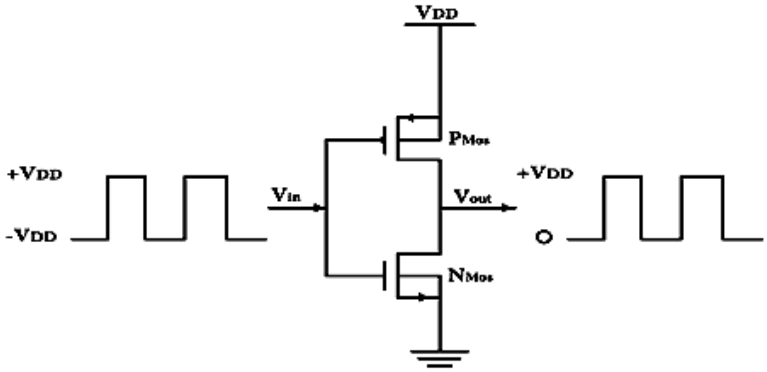

Fig. 3.6 Level shifter using the inverter.

3.4.3 Frequency Division Circuit:

The frequency division circuit consists of a D Flip Flop as shown in Fig.3.7 whose function is to reduce the output frequency of VCO by a factor of (1/K), where K is the frequency division ratio. Each stage from D Flip Flop divides the frequency by (2). So, we need 7 stages of D flip-flops to obtain the required frequency.

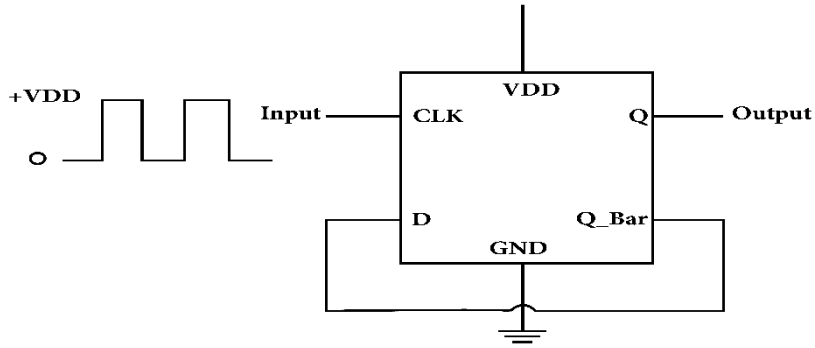

Fig. 3.7 Block diagram of D- Flip Flop circuit.

3.5 Simulation Results

The circuit is designed in 0.13-µm CMOS technology with ± 0.9 V supply voltage. TEAM memristor model is used for memristors [12,13]. Table 3.1 shows the dimensions of TiO2 memristor **[11]:**

Table 3.1: The dimensions of Tio2 Memristor [11]

	Length(L)	**Width(z)**	**Thickness(h)**
Thin-film	**50 nm**	**50 nm**	**10 nm**

The memristor area can be calculated as provided in equation (3.38):

$$A = L*Z \qquad (3.38)$$

where A is the area of the memristor, L is the length of the memristor and Z is the width of the memristor

Fig.3.8. shows the output signal for 185 Hz from the VCO that is produced by using (Vc = 0.2 V, R_{OFF}_M = 25KΩ, R_{OFF}_M1 = 40KΩ, R_{OFF}_M2 = 100 KΩ, C = 1nF, L+ = 0.9 V).

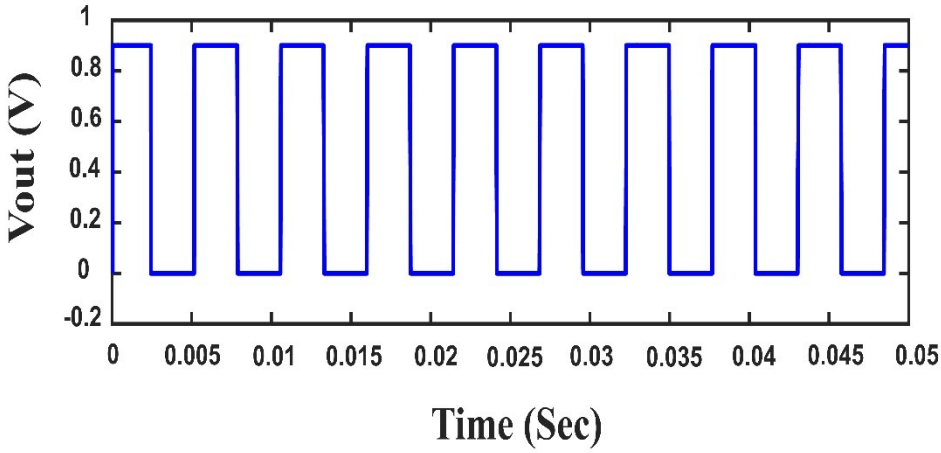

Fig. 3.8. VCO 185 Hz output signal

Fig.3.9. shows the output signal for 126 Hz from the VCO that is produced by using (Vc = 0.4 V, R_{OFF}_M = 25KΩ, R_{OFF}_M1 = 40KΩ, R_{OFF}_M2 = 100KΩ, C = 1nF, L+ = 0.9 V).

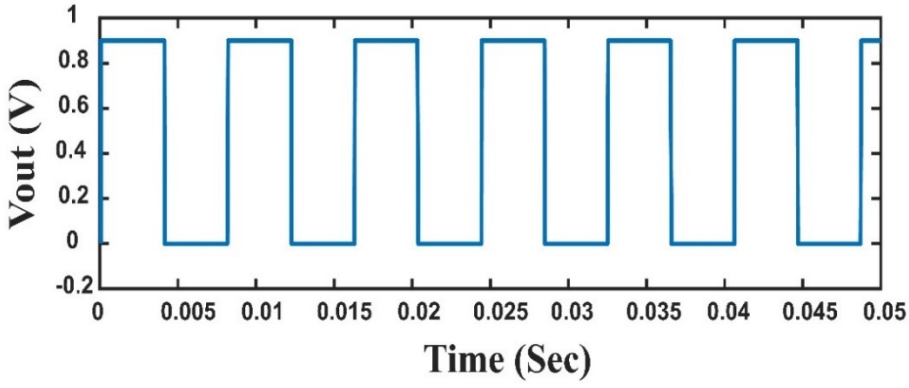

Fig. 3.9. VCO 126 Hz output signal

Fig.3.10. shows the output signal of 104 Hz from the VCO that is produced by using (Vc = 0.5 V, R_{OFF}_M = 25KΩ, R_{OFF}_M1 = 40KΩ, R_{OFF}_M2 = 100KΩ, C =1nF, L+ = 0.9 V).

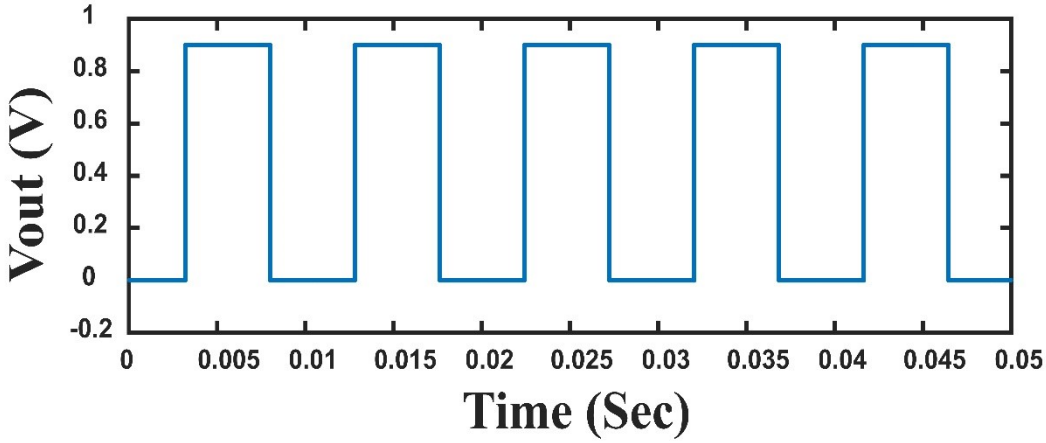

Fig. 3.10. VCO 104 Hz output signal

Fig.3.11. shows the output frequency range from 104 Hz to 203 Hz as the controlled voltage varies from 0.1 V to 0.5 V with a supply voltage (±0.9 V).

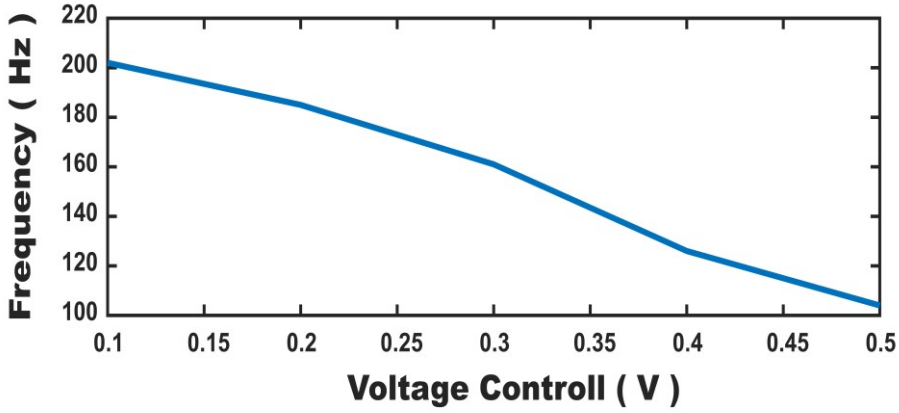

Fig. 3.11. Output frequency versus control voltage

A comparison between the proposed memristor based deep brain stimulation circuit and the other circuits in the literature are summarized in the following table 3.2.

Table 3.2: The Simulation Results with The Previous Work Reported Results

	Hwang et al. [10]	Veeravalli et al. [9]	M. Wang et al [11]	Proposed circuit
Minimum frequency (Hz)	0.3	0.2	0.03	104
Maximum frequency (Hz)	100	5.0	185	203
Tuning ratio	333: 1	25: 1	6167: 1	1.95: 1
DC supply voltage (V)	3.0	±1.5	1.2	±0.9
DC power dissipation	0.3 mW	5.57 µW	97.2 mW	0.79 mW
CMOS technology	2-µm	1.2-µm	0.13-µm	0.13-µm
Chip core area (mm2)	0.281	2.16	0.45	0.67

3.7 Conclusion

The proposed VCO circuit produces a low frequency that ranges from 104 Hz to 203 Hz which makes the proposed VCO circuit a very good candidate for low frequency applications (i.e., in the deep brain stimulation). Also, it achieves low power consumption in milliwatt (0.79

mW) which is considered the most important parameter in neural stimulator (i.e., in the deep brain stimulation) and should be low to avoid destroying brain cells. Also, it achieves a suitable low silicon area, the total area equal ($0.67mm^2$) and this makes the process of fabrication easier and not expensive. Even though the proposed circuit has a lower tuning ratio than the other works. However, the circuit achieves exactly the required frequency range for Parkinson's diseases from 130 Hz to 185 Hz.

A new Design technique for a low frequency voltage controlled oscillator circuit, using a memristor for deep brain stimulation, is presented. The proposed circuit achieves a frequency range from 104 Hz to 203 Hz with a low power consumption equals 0.79 mW which required in deep brain stimulators and the total silicon area equals 0.67 mm^2. The proposed circuit is used in deep brain stimulation and it's considered as a therapy of Parkinson's disease or cardiac tissue stimulation.

Chapter 4

Experimental Setup and Testing

4.1 Introduction

This chapter provides a hardware implementation of a memristors-based voltage controlled oscillator which is used in electrical neural stimulation. The basic proposed circuit generates low frequency signals that range from 1.2 KHz to 3.4 KHz with a small area and low power consumption about 0.49 mW. In addition, four-stages D-flip-flops are used as a frequency divider circuit to reduce the frequency range from KHz range to Hz range which is very useful in biomedical and embedded systems applications.

With respect to the fast development of the electronic industry, new devices have become increasingly important such as the memristor. This passive element was theorized and characterized by Prof Chen [1], [3]. It has many valuable characteristics such as non-volatility properties, high performance, high-density, nano-scale size, and low power device [48], [4]. It is useful for many modern small size applications such as nonvolatile memory, low power, remote sensing systems, neuromorphic applications, and analog computation [49].

Furthermore, this chapter is an extension of the previous work which was reported in a chapter (3). The hardware implementation details of the proposed VCO circuits are provided in Chapter 3. Also, this chapter gives the measurement results with a comparison between the resistors-based and memristors-based circuits as a verification.

Memristors have recently been fabricated by Knowm Inc Company for hardware applications [50].

4.2 Industrial Memristor

Knowm Inc is an American company that was founded in 2015 and worked toward neuro-memristive applications. In January 2018, the Knowm memristors have become available on the open-source memristor discovery platform [50].

The Knowm memristors, also known as the Knowm Self Directed Channel (SDC) memristors, come in three variants: Tungsten (W), Tin (Sn), and Chromium (Cr), which refers to the metal introduced in the active layer during fabrication. Each memristor type has the same basic material structure, but they differ in the active metal added to the active layer [50]. Tungsten (W) type has been used throughout this work and it is available in packaged devices as shown in Fig.4.1.

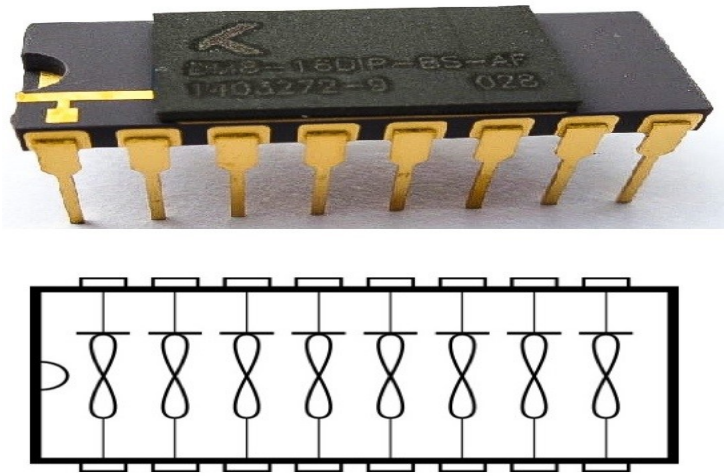

Fig. 4.1 Knowm Memristor Package [50]

The Knowm Multi-Stable Switch (MSS) model provides a description of an idealized two-state element that switches probabilistically between its two states as a function of applied voltage bias and temperature. A single memristor is modeled by a collection of MSSs states changing over time, which captures the memory-enabling hysteresis behavior [50].

The I-V relationship for Knowm memristor MSS model is shown in (4.1):

$$I = \emptyset I_m(\mathrm{V},\mathrm{T}) + (1-\emptyset) I_s(\mathrm{V}) \qquad (4.1)$$

where I is the total current, I_m is the memory-dependent current, I_s is a Schottky diode current. $\emptyset \in [0,1]$, a value of $\emptyset = 1$ represents a device and it does not contain a Schottky diode effect [8]. For more details in how to model I_m and I_s are addressed in [50].

The memristor programming to write a certain value of its state (resistance) is done by Knowm Kit along with analog discovery board and its software as shown in Fig.4.2.

Fig. 4.2 Memristor programming using Knowm Kit along with analog discovery board.

The attained memristor resistance cycles between high and low resistance values by switching the polarity of the applied potential across the device. Also, the attained memristor resistance depends on the value of the applied potential and its time duration. Therefore, the resistance value is related to the amount of metal located within the active layer, where the application of an external voltage causes the channel's transition between conducting and non-conducting states [9].

4.3 Experimental Setup

This section elicits the hardware implementation details of the proposed VCO circuits reported in Chapter (3). The basic hardware circuit schematic diagrams for both resistors-based and memristor-based VCO are shown in Fig.4.3.

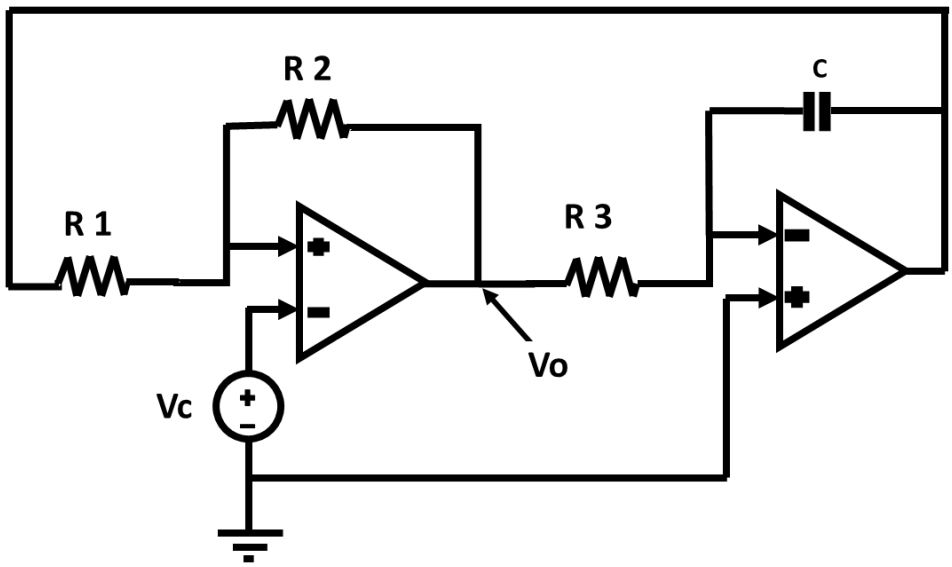

(a)

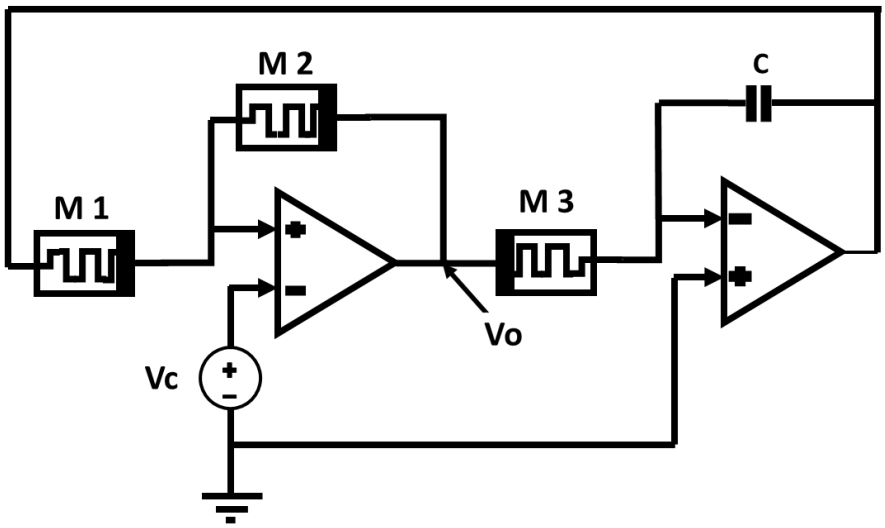

(b)

Fig. 4.3 basic hardware circuit schematic diagrams for (a) Resistors-based VCO circuit (b) Memristors-based VCO circuit

One of the key concepts in electronics is the Printed Circuit Board (PCB). Although, most PCBs for simple electronics are simple and they are composed of only a single layer. More sophisticated hardware such as computer graphics cards or motherboards can have multiple layers, and sometimes up to twelve. Although PCBs are be found in many other electronic devices, such as Medical devices.

Electronics products are now denser and they consume less power than the previous generations by making it possible to test new and exciting medical technology. Most medical devices use a high-density PCB, which is used to create the smallest and densest design possible. This helps to alleviate some of the unique constraints involved with developing devices for the medical field due to the necessity of small size and lightweight.

PCBs have found their way into everything from small devices, such as Neural Stimulation [site].

The PCB Wizard 3.50 Pro Unlimited program was used to design and to printed the basic hardware circuit schematic diagrams for both resistors-based and memristors-based VCO.

Fig.4.4. shows the complete stage of the printed circuit for implementing the power supply circuit from the design of the circuit to the printed circuit.

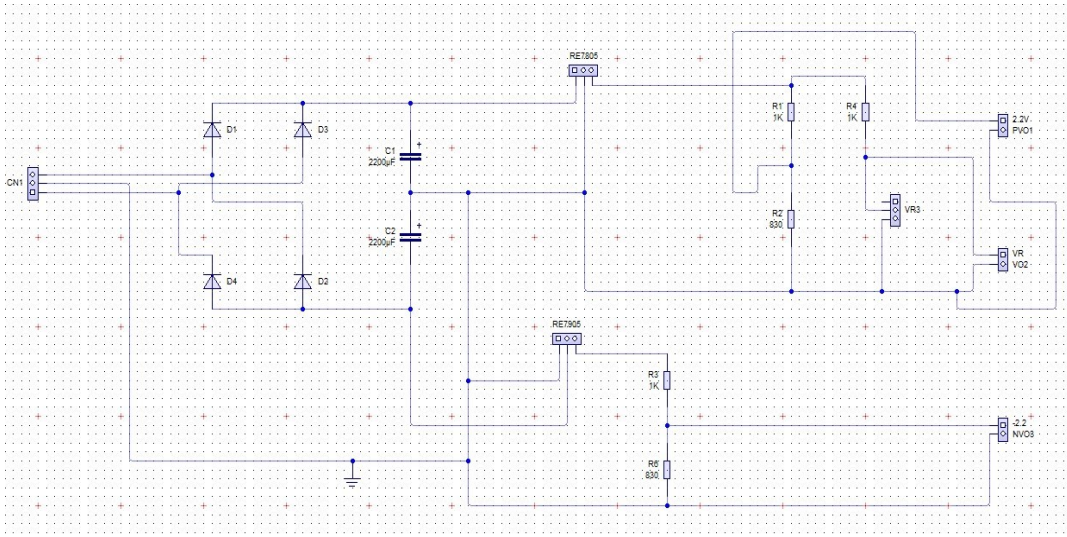

(a)

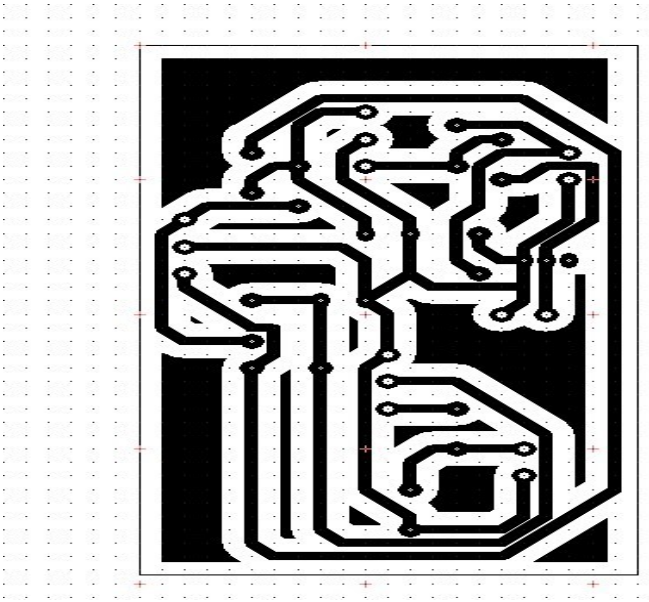

(b)

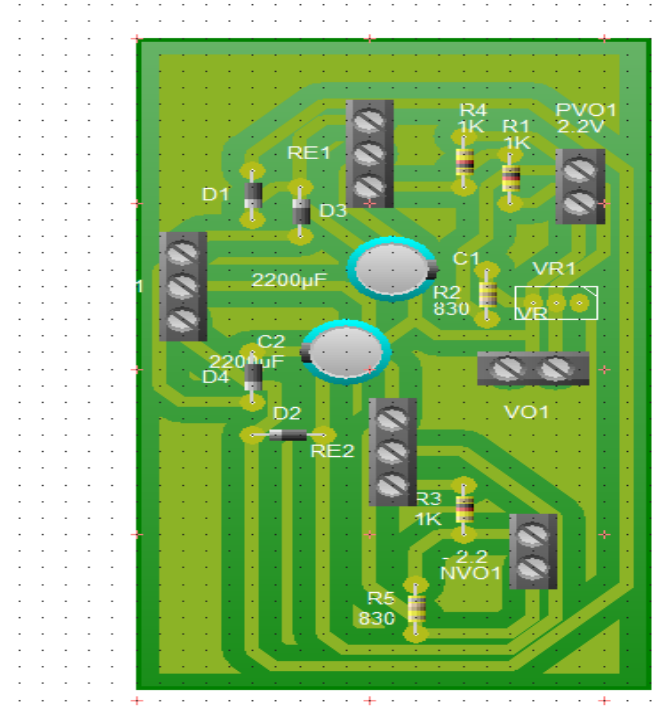
R4
1K
R1
1K
PVO1
2.2V
RE1
D1
D3
C1
2200µF
VR1
R2
830
VR
C2
220µF
D4
VO1
D2
RE2
R3
1K
2.2
NVO1
R5
830

(c)

Fig. 4.4 The complete stage of the printed circuit for implementing Power Supply (a) Design the circuit (b) Preparing the circuit for printing (c) The Final shape of the Circuit after Printed.

Fig.4.5. shows the complete stage of the printed circuit for implementing Resistors-based VCO circuit from the design of the circuit to the printed circuit. The low power dual operational amplifier (LM 358) is used in both Schmitt trigger and integrator implementations with ±2V supply voltage.

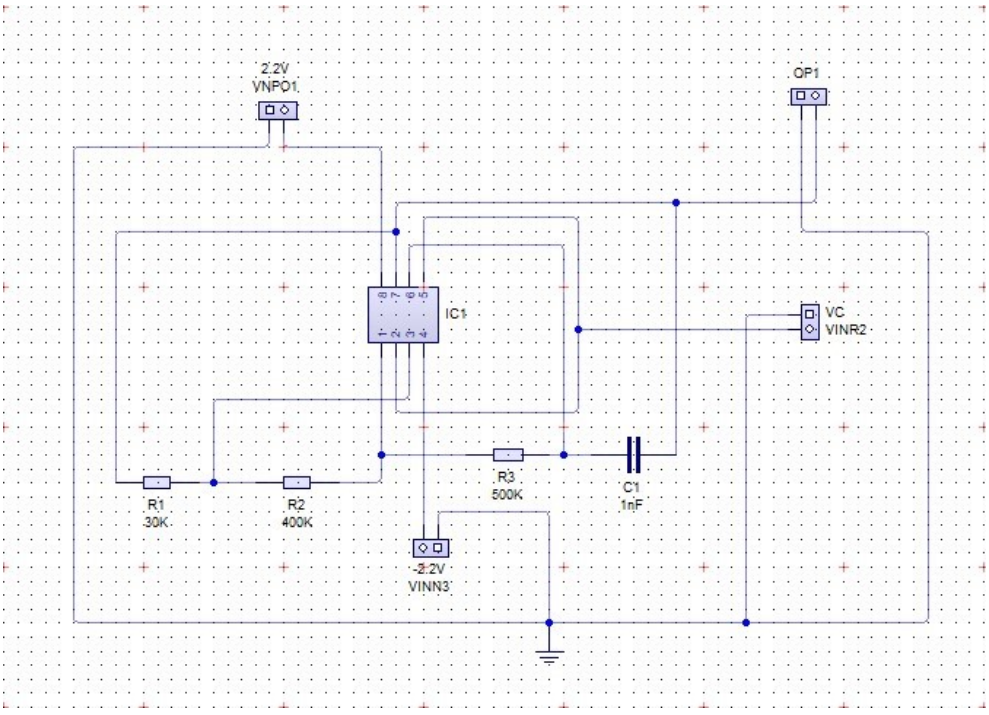

(a)

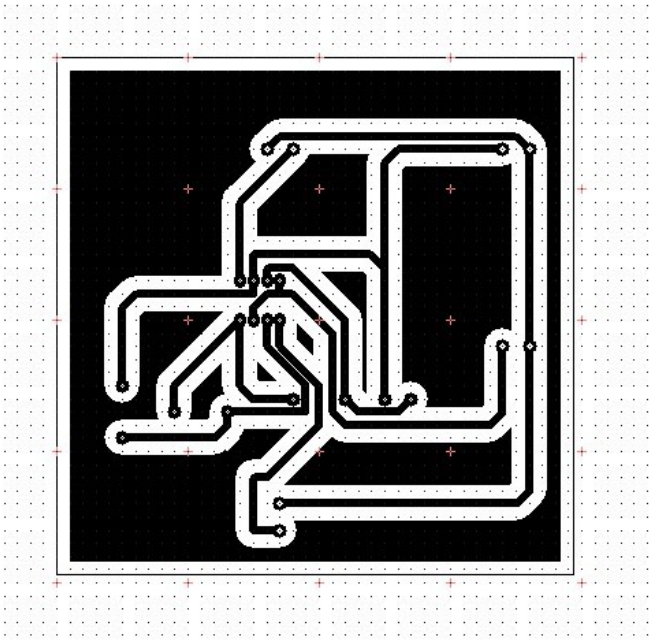

(b)

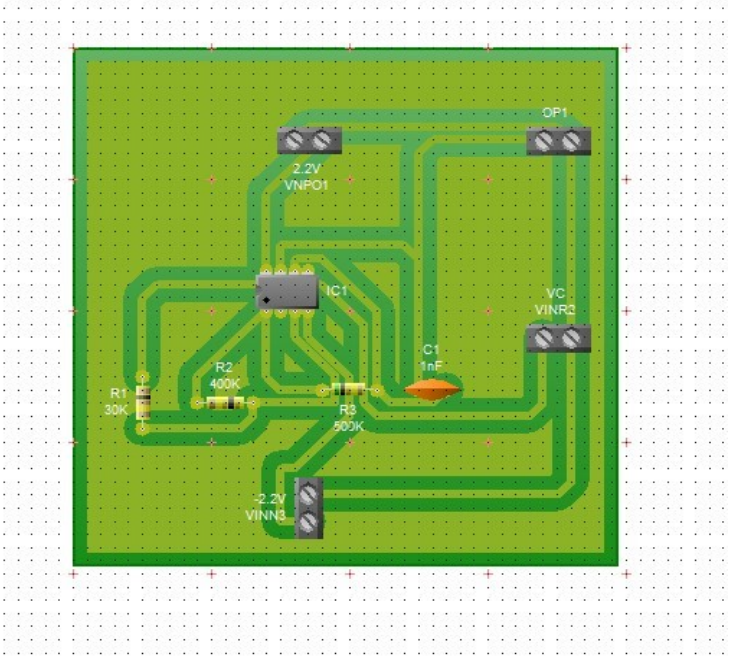
OP1
2.2V
VNPO1
IC1
VC
VINR2
C1
1nF
R2
400K
R1
30K
R3
500K
-2.2V
VINN3

(c)

Fig. 4.5 The complete stage of the printed circuit for implementing Resistors-based VCO circuit (a) Design the circuit (b) Preparing the circuit for printing (c) The Final shape of the Circuit after Printed.

Fig.4.6. shows the complete stage of the printed circuit for implementing the Memristor Kit from the design of the circuit to the printed circuit.

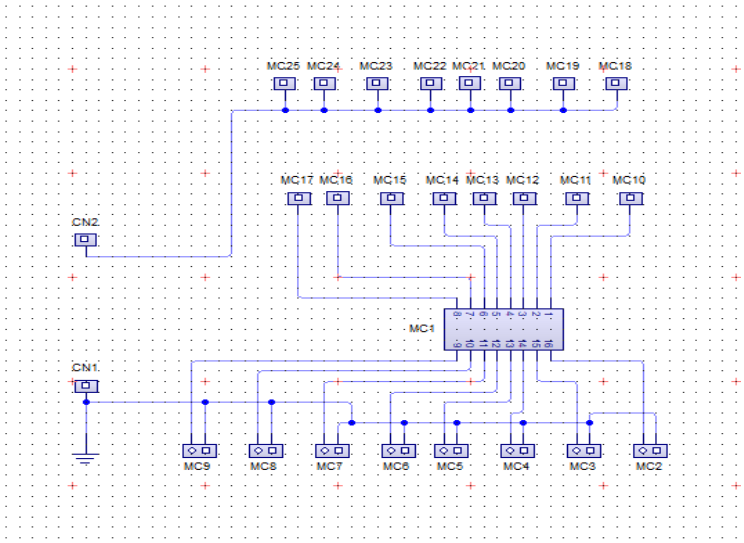

(a)

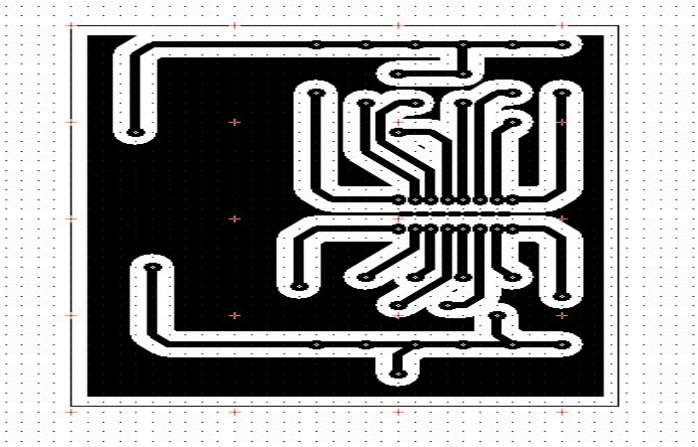

(b)

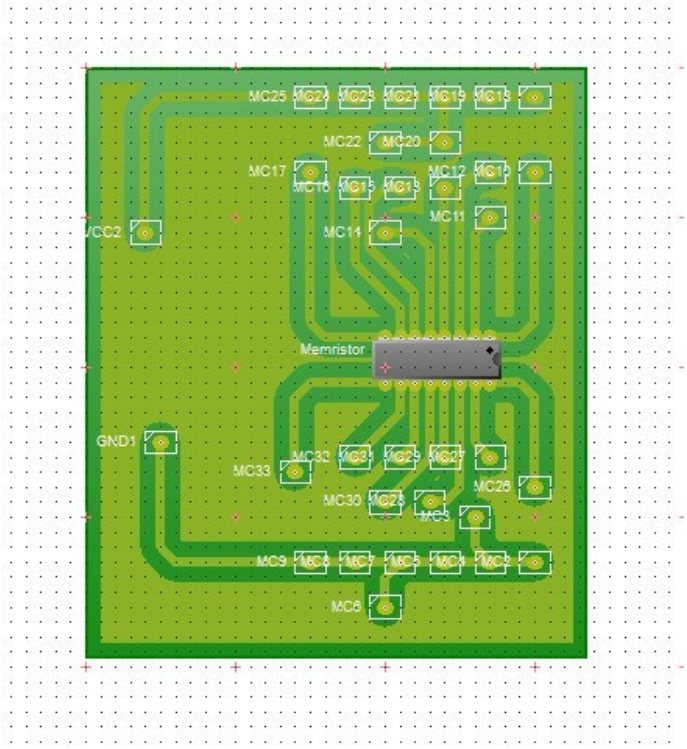

(c)

Fig. 4.6 The complete stage of the printed circuit for implementing Memristor Kit (a) Design the circuit (b) Preparing the circuit for printing (c) The Final shape of the Circuit after Printed.

Fig.4.7. shows the complete printed circuit boards (PCBs) arrangement for implementing the memristor-based VCO prototype circuit. This arrangement shows the implemented basic VCO circuit which consists of PCB power supply circuit, PCB Schmitt trigger, integrator circuit, and PCB memristor kit. The low power dual operational amplifier (LM 358) is used in both Schmitt trigger and integrator implementations.

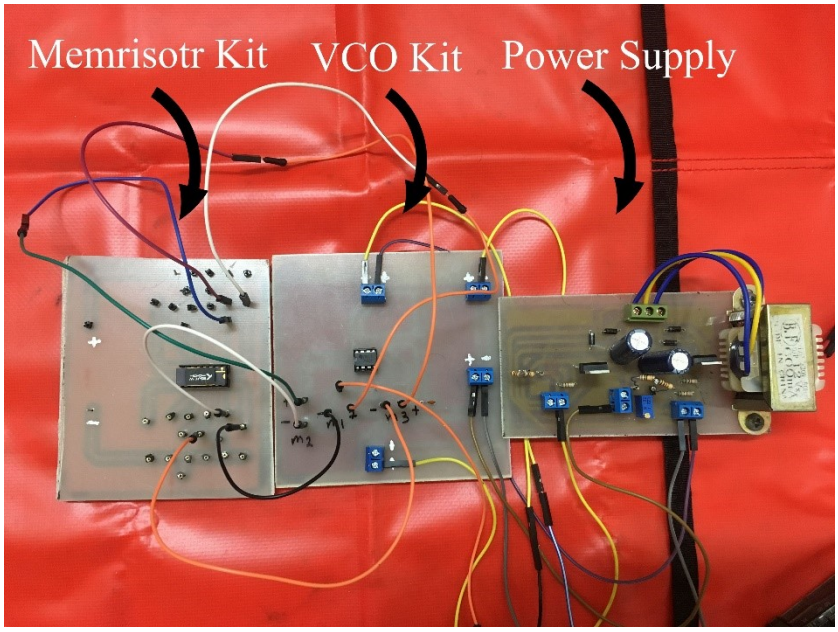

Fig. 4.7 The complete printed circuit boards (PCBs) arrangement for implementing the memristor-based VCO prototype circuit.

Fig.4.8. shows the complete printed circuit boards (PCBs) arrangement for implementing the Resistor-based VCO prototype circuit.

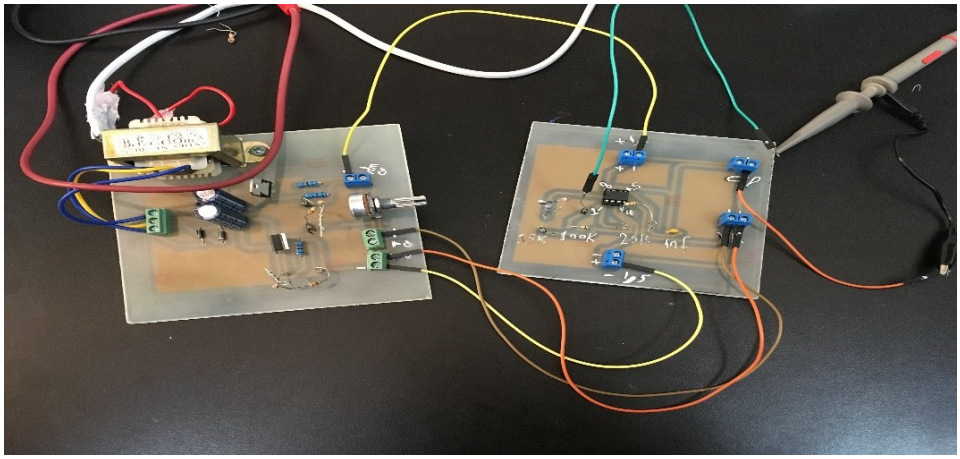

Fig. 4.8 The complete printed circuit boards (PCBs) arrangement for implementing the Resistor-based VCO prototype circuit.

The hardware implementation of the VCO system is achieved by using the commercially available Knowm memristor kit and integrated circuits in combination with the necessary discrete components.

The output of the implemented VCO is connected to the Digilent Analog Discovery2 through its pinouts as shown in Fig.4.9. [51], and it is used as an oscilloscope. Digilent Analog Discovery2 is a multi-function instrument that allows users to measure visualize, generate, record, and control mixed signal circuits of all kinds [51].

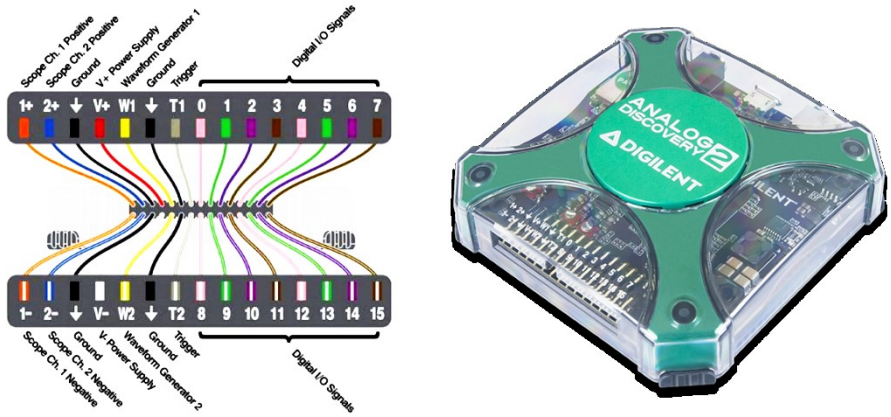

Fig. 4.9 The Digilent Analog Discovery2 and Reference Manual

4.4 Experimental Results

In this section, the VCO outputs for the practical implementation of VCO circuit are illustrated for both resistors-based and memristor-based VCO for different values of Vc.

4.4.1 Resistors – Based VCO:

The resistors-based VCO circuit, as shown in Fig.4.3. (a) is implemented with the values of the three resistors: (R_1 = 30 KΩ, R_2 = 400 KΩ, and R_3 = 500 KΩ), and the capacitance value (C = 1nF). The control voltage (Vc) value is swept from 0.1 V to 0.45 V with step 0,05 V. The VCO output is displayed by using Analog Discovery 2 as an oscilloscope.

Fig.4.10. shows the output signal for VCO versus time in which the value of the control voltage (Vc) equals (0.1) V and the output signal frequency equals 2.9 kHz.

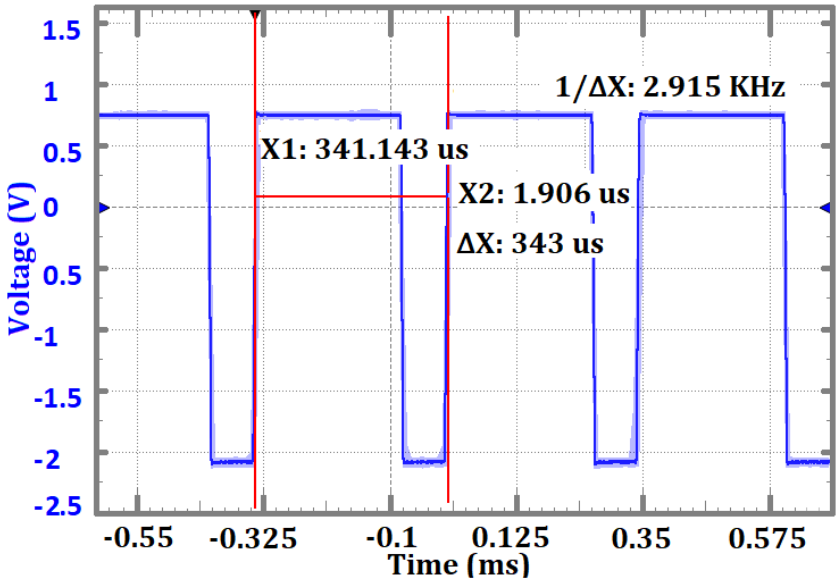

Fig. 4.10 Output signal with frequency =2.9 KHz for Vc = 0.1 V.

Fig.4.11. shows the output signal for VCO versus time in which the value of the control voltage (Vc) equals (0.35) V and the output signal frequency equals 2 kHz.

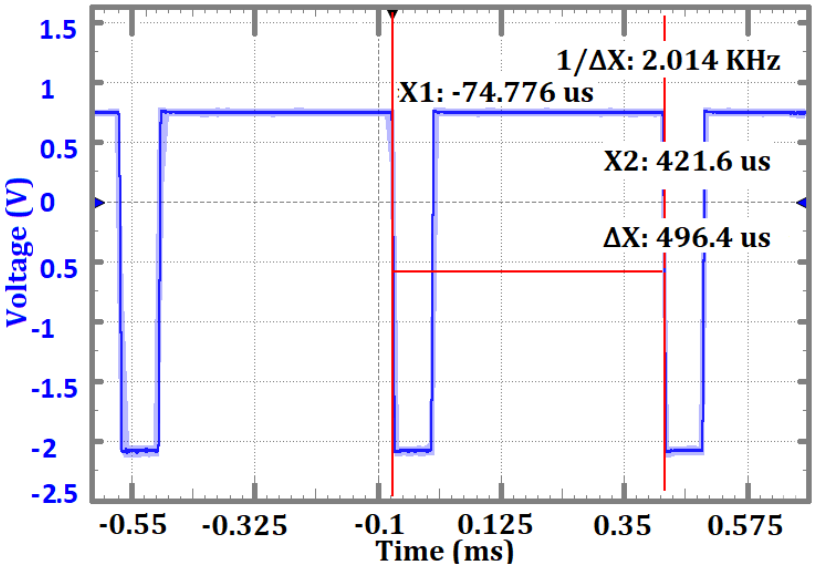

Fig. 4.11 Output signal with frequency =2.0 KHz for Vc = 0.35 V.

Fig.4.12. shows the output signal for VCO versus time in which the value of the control voltage (Vc) equals (0.45) V and the output signal frequency equals 1.5 kHz.

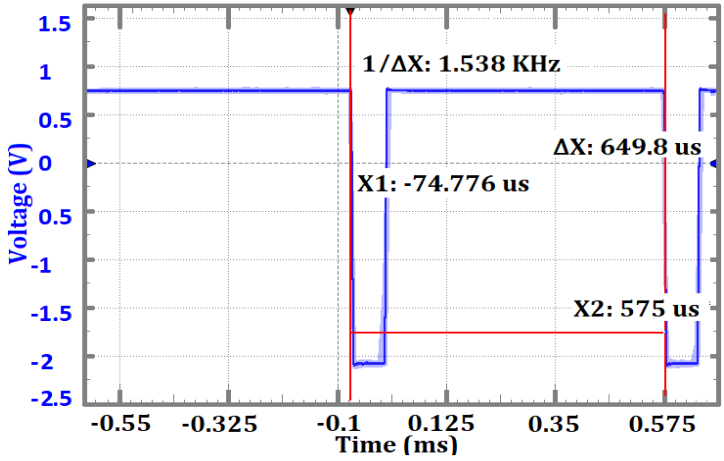

Fig. 4.12 Output signal with frequency =1.5 KHz for Vc = 0.45 V.

4.4.2 Memristors – Based VCO

The memristors-based VCO circuit which is shown in Fig.4.3. (b) is implemented with the values of the three memristors are programmed as

(M1 = 30 KΩ, M2 = 400 KΩ, and M3 = 500 KΩ), and the capacitance value (C = 1nF). Also, the control voltage (Vc) value is swiped from 0.1 V to 0.45 V with step 0.05 V.

Fig.4.13. shows the output signal for VCO versus time in which the value of the control voltage (Vc) equals (0.1) V and the output signal frequency equals 3.4 kHz.

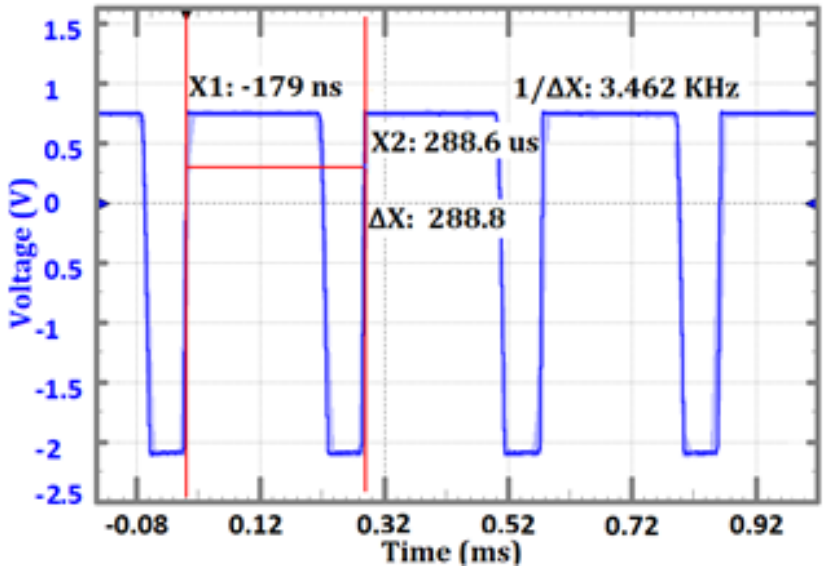

Fig. 4.13 Output signal with frequency =3.4 KHz for Vc = 0.1 V.

Fig.4.14. shows the output signal for VCO versus time in which the value of the control voltage (Vc) equals (0.35) V and the output signal frequency equals 1.6 kHz.

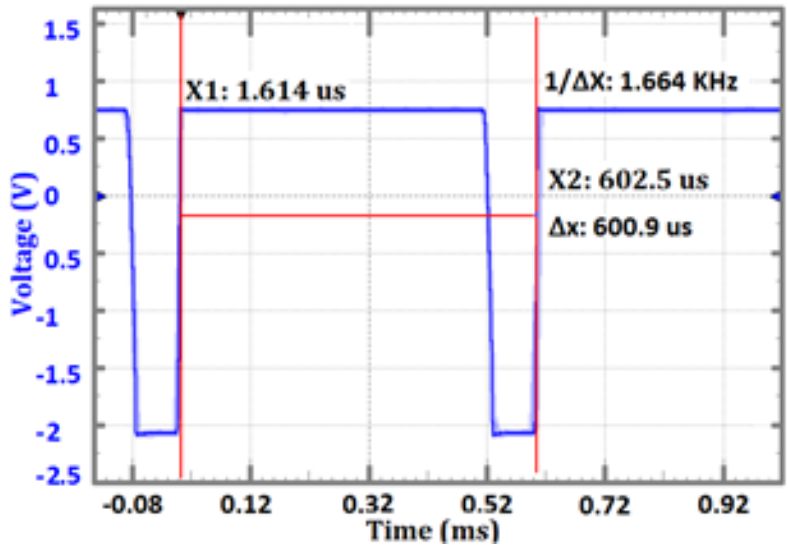

Fig. 4.14 Output signal with frequency =1.6 KHz for Vc = 0.35 V.

Fig.4.15. shows the output signal for VCO versus time in which the value of the control voltage (Vc) equals (0.45) V and the output signal frequency equals 1.19 kHz

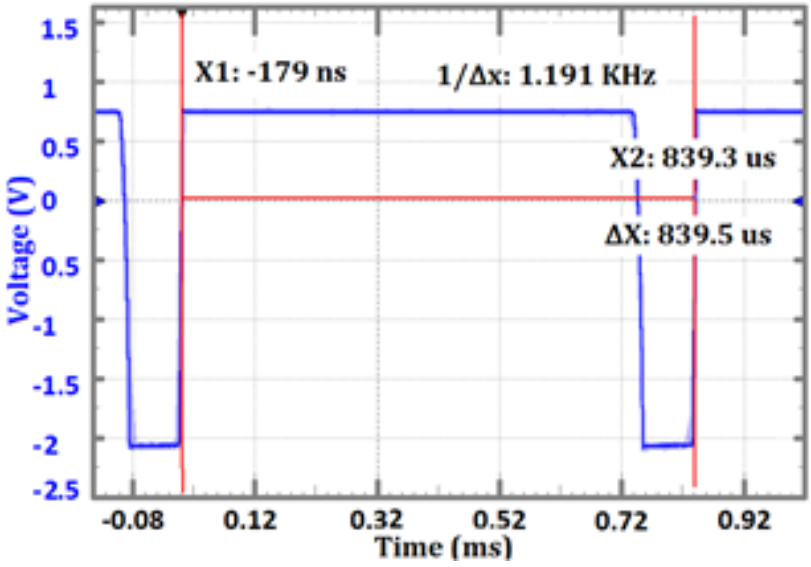

Fig. 4.15 Output signal with frequency =1.19 KHz for Vc = 0.45 V.

Fig.4.16. shows a comparison for the possible full range of VCO frequencies for both memristor-based and resistor-based VCOs. The VCO is restricted in this range due to the selected resistor values. As shown, there is a fair agreement between the two designs and the worst deviation in the full frequency range is about 0.5 KHz.

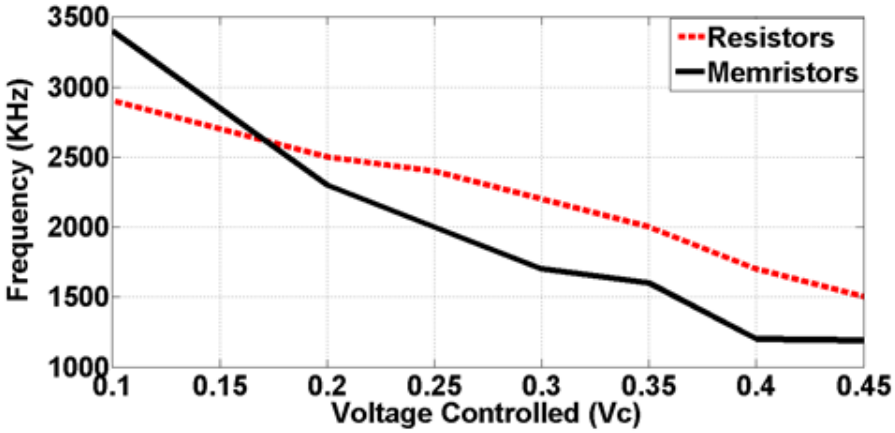

Fig. 4.16 Output oscillation frequency versus the controlled voltage for resistors-based and memristors-based VCO.

Finally, a frequency divider consists of a number of D-flip-flops stages that can be used to reduce the VCO frequency (i.e., kHz range) to very low frequency (i.e., Hz range), which is very useful for the deep brain stimulation. The number of D-flip-flops stages depends on the required frequency reduction ratio.

4.6 Conclusion

A Hardware prototype of a memristors-based low frequency voltage-controlled oscillator circuit is implemented and compared with resistors-based one with the same circuit structure. There is a fair agreement between the two designs and the worst deviation in the full frequency range is about 0.5 KHz. The implemented prototype achieves a frequency range from 1.2

KHz to 3.4 KHz with low power consumption equals 0.49 mW and achieves a low silicon area compared to the passive elements.

Chapter 5

Conclusions and Future Work

This chapter presents a brief summary of the thesis. Moreover, the chapter highlights the main conclusion and give some recommendation for future work.

5.1 Brief Summary

The main objective of this thesis is to design and to implement a low-frequency voltage controlled oscillator in order to achieve a wide tuning range with a practical small area and low power constraints to use this VCO in neural stimulation. Neural stimulation is considered as one of the most important stimulations in biomedical engineering because it is used to treat the chronic pain such as Parkinson's disease. This objective was achieved by using memristors because the memristor has two important advantages to be used in the voltage-controlled oscillator design for electrical neural stimulation which are: nano scale dimensions and low power consumption. A new design technique for a low-frequency voltage controlled oscillator circuit using a memristor for deep brain stimulation is presented by simulation and hardware implementation.

5.2 Conclusion

The main conclusion of this thesis can be listed as follows:

- A comprehensive review of the types and the models of memristors have been explained. Also, the memristor applications are illustrated.

- The voltage-controlled oscillator operating principle and its applications are discussed. Also, biomedical applications and its required frequency range are reviewed.
- A new Design technique for a low-frequency voltage controlled oscillator circuit, using a memristor for deep brain stimulation, is applied.
- Simulation of the memristor based new voltage-controlled oscillator for electrical neural stimulation using Cadence is presented.
- The proposed circuit generates low frequency range from 104 Hz to 203 Hz with a low power consumption equal 0.79 mW which is the main challenge in deep brain stimulators, and the total silicon area is 0.67 mm^2.
- A comparison between the proposed circuit with a memristor based deep brain stimulation circuit and other circuits is presented.
- The hardware prototype of a memristors-based low frequency voltage-controlled oscillator circuit is provided. The basic proposed circuit generates low frequency signals that range from 1.2 KHz to 3.4 KHz with a small area and low power consumption about 0.49 mW.
- The measurement results were involved with a comparison between the resistors-based and memristors-based circuits as a verification process.

5.3 Future Work

Based on this work, some perspectives for future work are suggested as follows:

- The fabricated area of the proposed VCO circuit can be effectively reduced further by using a capacitor-less integrator by replacing the conventional capacitance by nanoscale memcapacitance circuits.
- Refresh circuit for the memristors used in the VCO could be added to maintain the resistance value after several periods of operation.

Publication Extracted from the Thesis

A large portion of the work completed in this thesis has been published in or submitted to:

[1] M. I. Selmy, H. Mostafa, and A. A. S. Dessouki, "Low Power Memristor Based Voltage Controlled Oscillator for Electrical Neural Stimulation", IEEE International Conference on Advanced Control Circuits and Systems and New Paradigms in Electronics & Information Technology (ACCS/PEIT 2017), Alexandria, Egypt, pp. 344 – 347, 2017.

DOI: 10.1109/ACCS-PEIT.2017.8303063

URL: https://ieeexplore.ieee.org/document/8303063

[2] M. I. Selmy, H. Mostafa, and A. A. S. Dessouki, "Hardware Implementation of a Low Power Memristor Based Voltage Controlled Oscillator", IEEE International Conference on Microelectronics (ICM 2019), Cairo, Egypt.

[Submitted]

References

[1] L. Chua, "Memristor-the missing circuit element," IEEE Transactions on Circuit Theory, vol. 18, pp. 507-519, 1971.

[2] M. Di Ventra, Y. V. Pershin, and L. O. Chua, "Circuit elements with memory: memristors, memcapacitors, and meminductors," Proceedings of the IEEE, vol. 97, pp. 1717-1724, 2009.

[3] D. B. Strukov, G. S. Snider, D. R. Stewart, and R. S. Williams, "The missing memristor found," Nature, vol. 453, p. 80, 2008.

[4] Elshamy, Mohamed, Hassan Mostafa, and M. Sameh Said. "Comparative review of the TiO2 and the spintronic memristor devices." IEEE 27th Canadian Conference on Electrical and Computer Engineering (CCECE), 2014.

[5] Mohamed Elshamy, "Design of Read/Write Circuits Suitable for Memristor-Based Memory Arrays", Cairo University. Co-supervised by Prof. M. Sameh Said.

[6] R. S. Williams. How we found the missing memristor. in IEEE Spectrum. 45, no. 12,pp. 28-35, December 2008.

[7] [Online]Available: https://www.theregister.co.uk/Print/2011/12/27/memristors_and_mouttet/

[Accessed: 30 Feb. 2020].

[8] L. Wang, C. Yang, J. Wen, S. Gai, and Y. Peng, "Overview of emerging memristor families from resistive memristor to spintronic memristor," Journal of Materials Science: Materials in Electronics, vol. 26, pp. 4618-4628, 2015.

[9] A. Kumar and M. Baghini, "Experimental study for selection of electrode material for ZnO-based memristors," Electronics Letters, vol. 50, pp. 1547-1549, 2014.

[10] A. C. Torrezan, J. P. Strachan, G. Medeiros-Ribeiro, and R. S. Williams, "Sub-nanosecond switching of a tantalum oxide memristor," Nanotechnology, vol. 22, p. 485203, 2011.

[11] X. Wang, Y. Chen, H. Xi, H. Li, and D. Dimitrov, "Spintronic memristor through spin-torque-induced magnetization motion," IEEE electron device letters, vol. 30, pp. 294-297, 2009.

[12] C. Xu, X. Dong, N. P. Jouppi, and Y. Xie, "Design implications of memristor-based RRAM cross-point structures," in Design, Automation & Test in Europe Conference & Exhibition (DATE), Grenoble, France, pp. 1-6, 2011.

[13] Y. Ho, G. M. Huang, and P. Li, "Dynamical properties and design analysis for nonvolatile memristor memories," IEEE Transactions on Circuits and Systems I: Regular Papers, vol. 58, pp. 724-736, 2011.

[14] I. E. Ebong and P. Mazumder, "CMOS and memristor-based neural network design for position detection," Proceedings of the IEEE, vol. 100, pp. 2050-2060, 2012.

[15] A. Wu and Z. Zeng, "Dynamic behaviors of memristor-based recurrent neural networks with time-varying delays," Neural Networks, vol. 36, pp. 1-10, 2012.

[16] S. Kvatinsky, A. Kolodny, U. C. Weiser, and E. G. Friedman, "Memristor-based IMPLY logic design procedure," in IEEE 29th International Conference on Computer Design (ICCD), Amherst, MA, USA, pp. 142-147, 2011.

[17] W. Wang, T. T. Jing, and B. Butcher, "FPGA based on integration of memristors and CMOS devices," in Proceedings of 2010 IEEE International Symposium on Circuits and Systems (ISCAS), 2010, pp. 1963-1966.

[18] J. Rajendran, H. Manem, R. Karri, and G. S. Rose, "Memristor based programmable threshold logic array," in Proceedings of the 2010 IEEE/ACM International Symposium on Nanoscale Architectures, 2010, pp. 5-10.

[19] A. Chanthbouala, V. Garcia, R. O. Cherifi, K. Bouzehouane, S. Fusil, X. Moya, et al., "A ferroelectric memristor," Nature Materials, vol. 11, pp. 860-864, 2012

[20] D. Liu, H. Cheng, X. Zhu, G. Wang, and N. Wang, "Analog memristors based on thickening/thinning of Ag nanofilaments in amorphous manganite thin films," ACS Applied Materials & Interfaces, vol. 5, pp. 11258-11264, 2013.

[21] S. Benderli and T. Wey, "On SPICE macromodelling of TiO2 memristors," Electronics Letters, vol. 45, pp. 377-379, 2009.

[22] Y. N. Joglekar and S. J. Wolf, "The elusive memristor: properties of basic electrical circuits," European Journal of Physics, vol. 30, p. 661, 2009

[23] Z. Biolek, D. Biolek, and V. Biolkova, "SPICE model of memristor with nonlinear dopant drift," Radioengineering, vol. 18, pp. 210-214, 2009.

[24] M. D. Pickett, D. B. Strukov, J. L. Borghetti, J. J. Yang, G. S. Snider, D. R. Stewart, et al., "Switching dynamics in titanium dioxide memristive devices," Journal of Applied Physics, vol. 106, pp. 074508-074508-6, 2009

[25] S. Kvatinsky, E. G. Friedman, A. Kolodny, and U. C. Weiser, "TEAM: Threshold adaptive memristor model," IEEE Transactions on Circuits and Systems I: Regular Papers, vol. 60, pp. 211-221, 2013.

[26] S. Kvatinsky, M. Ramadan, E. Friedman and A. Kolodny, VTEAM: A General Model for Voltage-Controlled Memristors, IEEE Transactions on Circuits and Systems II: Express Briefs, vol. 62, no. 8, pp. 786-790, 2015.

[27] S. Kvatinsky, K. Talisveyberg, D. Fliter, E. G. Friedman, A. Kolodny, and U. C. Weiser, "Verilog-A for memristor models," CCIT Technical Report, vol. 801, 2011

[28] Y. Chen and X. Wang, "Compact modeling and corner analysis of spintronic memristor," in Proceedings of the International Symposium on Nanoscale Architectures IEEE/ACM, pp. 7-12, 2009.

[29] M. Hu, H. Li, Y. Chen, X. Wang, and R. E. Pino, "Geometry variations analysis of TiO 2 thin-film and spintronic memristors," in Proceedings of the 16th Asia and South Pacific design automation conference, Yokohama, Japan, pp. 25-30, 2011.

[30] P. Rabbani, R. Dehghani, and N. Shahpari, "A multilevel memristor– CMOS memory cell as a RERAM," Microelectronics J., vol. 46, no. 12, pp. 1283–1290, 2015.

[31] P. Mazumder, S. M. Kang, and R. Waser. Memristors: Devices, Models, and Applications.Proceedings of the IEEE, vol. 100, no. 6, pp. 1911-1919, 2012.

[32] Waser, Rainer and Ielmini, Daniele and Akinaga, Hiro and Shima, Hisashi and Wong, H-S Philip and Yang, Joshua J and Yu, Simon. Introduction to nanoionic elements for information technology. Resistive Switching: From Fundamentals of Nanoionic Redox Processes to Memristive Device Applications, 1-30,2016

[33] M. Shahsavari and P. Boulet, "Parameter Exploration to Improve Performance of Memristor-Based Neuromorphic Architectures," IEEE Transactions on Multi-Scale Computing Systems, vol. PP, no. 99, pp. 1– 1, 2017.

[34] H. G. Hezayyin, G. M. Ahmed, M. E. Fouda, L. A. Said, A. H. Madian, and A. G. Radwan, "A generalized family of memristor-based voltage controlled relaxation oscillator," International Journal of Circuit Theory and Applications, 2018.

[35] [Online]Available: https://www.electrical4u.com/voltage-controlled-oscillator/

[Accessed: 29 Feb. 2020].

[36] [Online]Available:https://www.electronicshub.org/voltage-controlled-oscillators-vco/ [Accessed: 29 Feb. 2020].

[37] Kackar, T.; Suman, S.; Ghosh, P. K. “Differential voltage controlled ring oscillators—A review,” Proc. of Int. Conf. on Communication and Networks, Vol. 508, p. 571-579,2017.

[38] O. Olabode, A. Ontronen, V. Unnikrishnan, M. Kosunen and J. Ryynänen, "A VCO-based ADC with Relaxation Oscillator for Biomedical Applications," 2018 25th IEEE International Conference on Electronics, Circuits and Systems (ICECS), Bordeaux, pp. 861-864, 2018.

[39] Xiang C, Zhang Y, Guo W, Liang XJ. Biomimetic carbon nanotubes for neurological disease therapeutics as inherent medication. Acta Pharm Sin B 2019.

[40] H. Feng, C. Zhao, P. Tan, R. Liu, X. Chen, Z. Li, Nanogenerator for biomedical applications, Adv. Healthc. Mater. 7 (2018) 1701298

[41] Anderson, Dustin, Grayson Beecher, and Fang Ba. "Deep brain stimulation in Parkinson’s disease: new and emerging targets for refractory motor and nonmotor symptoms." Parkinson’s disease 2017 (2017).

[42] [Online]Available: https://en.wikipedia.org/wiki/Pathophysiology_of_Parkinson%27s_disease [Accessed: 29 Feb. 2020].

[43] D. Su et al., “Frequency-dependent effects of subthalamic deep brain stimulation on motor symptoms in Parkinson’s disease: a metaanalysis of controlled trials,” Sci. Rep., vol. 8, no. 1, Dec. 2018.

[44] Limousin, Patricia, et al. "Electrical stimulation of the subthalamic nucleus in advanced Parkinson's disease." New England Journal of Medicine 339.16 (1998): 1105-1111.

[45] Veeravalli, Anand, Edgar Sánchez-Sinencio, and José Silva-Martínez. "A CMOS transconductance amplifier architecture with wide tuning range for very low frequency applications." IEEE Journal of Solid-State Circuits 37.6 (2002): 776-781.

[46] Hwang, Changku, et al. "A very low frequency, micropower, low voltage CMOS oscillator for noncardiac pacemakers." IEEE Transactions on Circuits and Systems I: Fundamental Theory and Applications 42.11 (1995): 962-966.

[47] Wang, Min, and Carlos E. Saavedra. "Very low frequency tunable signal generator for neural and cardiac cell stimulation." International Journal of Electronics 98.9 (2011): 12

[48] Nafea, Sherif F., et al. "Read disturbance and temperature variation aware spintronic memristor model," 2016 IEEE Canadian Conference on Electrical and Computer Engineering (CCECE2016), Vancouver, BC, Canada, May 2016, pp. 1-4.

[49] Kirar, Vishnu Pratap Singh, "Memristor: the missing circuit element and its application," World Academy of Science, Engineering and Technology, International Journal of Electrical, Computer, Energetic, Electronic and Communication Engineering, vol. 6, no. 12, pp. 1395-1397, 2012.

[50] Alex Nugent, "Self Directed Channel Memristors," Knowm Inc, April 2019.

[51] Digilent Inc., "Analog Discovery 2™ Reference Manual," Revised September 14, 2015.

Appendix A

Knowm Data Sheet [50]

A.1 Knowm Memristor:

The Knowm Memristor devices operate primarily through the mechanism of electric field induced generation and movement of metal ions through a multilayer chalcogenide material stack. A secondary mechanism of operation is phase-change, which can be selected as the primary mode of operation depending upon the operating conditions.

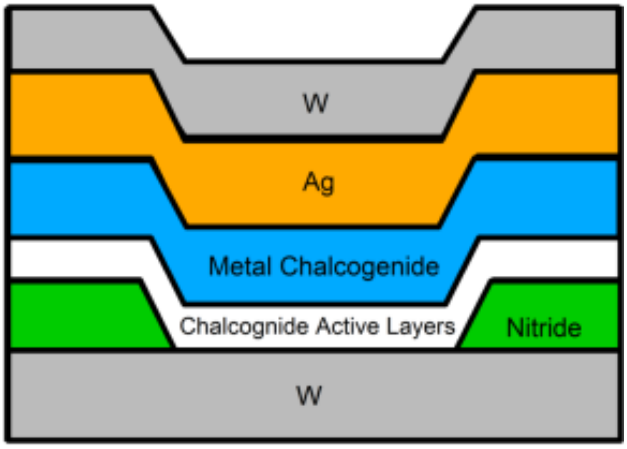

Knowm Memristor Material Stack

The Knowm Memristor come in three variants: W, Sn and Cr, which refers to the metal introduced in the active layer during fabrication. Each device is available in both raw die and packaged devices.

The research die was created to allow study of device operation over a wide range of device sizes. The die is 7860 μm by 5760 μm and consists of 9 columns of devices, each corresponding to a different device size. The size is listed at the bottom of each column. Each column contains 20 rows of each device size per column, for a total of180 devices.

Raw Die

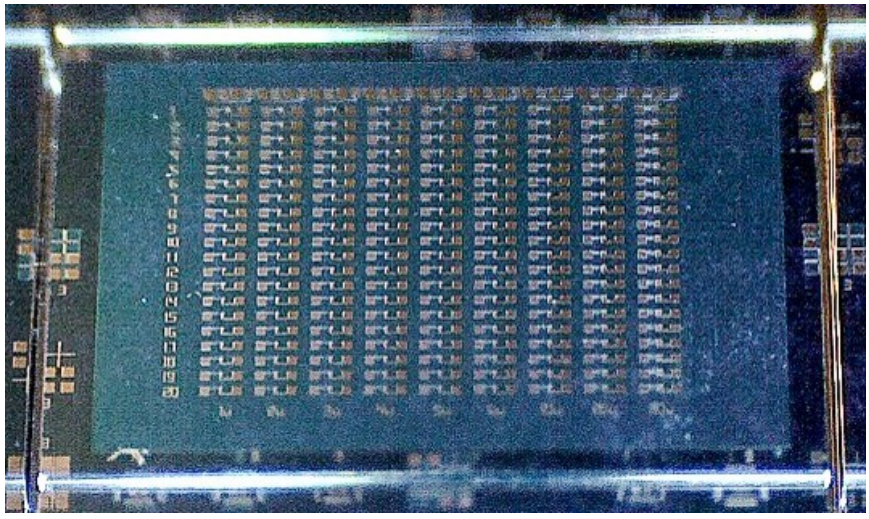

There are three different memristor material types available in the research die:

1- GeSeW (the ‘W’ device)

2- GeSeSn (the ‘Sn’ device)

3- GeSeCr (the ‘Cr’ device)

A.2 DC Response:

Cr (Chromium) Raw Die

Characteristic	Condition	Min	Type	Max	Std
Forward Adaptation Threshold	DC / quasi-static	0.220 V	0.332 V	0.560 V	0.089 V
Reverse Adaptation Threshold	DC / quasi-static	– 0.660 V	– 0.189 V	– 0.040 V	0.154 V
Cycle Endurance	1.5 Vpp, 500 Hz sine wave, 50 kΩ Series resistor	1M	50M	100M	
Low Resistance State	100nA Write Compliance Current	5.48E6 Ω	2.62E7 Ω	4.33E7 Ω	1.25E7 Ω
High Resistance State	100nA Write Compliance Current	1.07E11 Ω	1.59E12 Ω	9.00E12 Ω	2.62E12 Ω
Low Resistance State	1uA Write Compliance Current	1.51E5 Ω	1.90E6 Ω	1.04E7 Ω	2.87E6 Ω
High Resistance State	1uA Write Compliance Current	7.41E7 Ω	1.88E11 Ω	7.63E11 Ω	2.51E11 Ω
Low Resistance State	10uA Write Compliance Current	3.29E4 Ω	5.67E4 Ω	9.90E4 Ω	2.23E4 Ω

High Resistance State	10uA Write Compliance Current	2.53E7 Ω	1.14E11 Ω	1.00E12 Ω	2.96E11 Ω
Low Resistance State	100uA Write Compliance Current	2.65E3 Ω	4.82E3 Ω	1.05E4 Ω	2.09E3 Ω
High Resistance State	100uA Write Compliance Current	3.40E5 Ω	9.54E6 Ω	6.17E7 Ω	1.80E7 Ω
Low Resistance State	1mA Write Compliance Current	3.86E2 Ω	6.63E2 Ω	9.59E2 Ω	1.81E2 Ω
High Resistance State	1mA Write Compliance Current	3.63E4 Ω	7.49E4 Ω	1.49E5 Ω	4.04E4 Ω

Sn (Tin) Raw Die

Characteristic	Condition	Min	Type	Max	Std
Forward Adaptation Threshold	DC / quasi-static	0.150 V	0.259 V	0.340 V	0.042 V
Reverse Adaptation Threshold	DC / quasi-static	–0.230 V	–0.094 V	–0.030 V	0.053 V
Cycle Endurance	1.5 Vpp, 500 Hz sine wave, 50 kΩ Series resistor	50M	100M	5B	

Low Resistance State	100nA Write Compliance Current	7.41E5 Ω	7.17E6 Ω	3.56E7 Ω	9.87E6 Ω
High Resistance State	100nA Write Compliance Current	1.64E9 Ω	9.81E11 Ω	8.00E12 Ω	2.35E12 Ω
Low Resistance State	1uA Write Compliance Current	2.50E5 Ω	1.58E7 Ω	3.79E7 Ω	1.53E7 Ω
High Resistance State	1uA Write Compliance Current	7.60E6 Ω	2.23E11 Ω	1.43E12 Ω	4.10E11 Ω
Low Resistance State	10uA Write Compliance Current	3.14E4 Ω	1.57E5 Ω	1.16E6 Ω	3.33E5 Ω
High Resistance State	10uA Write Compliance Current	3.26E6 Ω	5.21E10 Ω	3.16E11 Ω	1.04E11 Ω
Low Resistance State	100uA Write Compliance Current	1.75E3 Ω	4.62E3 Ω	1.05E4 Ω	2.90E3 Ω
High Resistance State	100uA Write Compliance Current	5.64E5 Ω	5.80E10 Ω	2.50E11 Ω	8.22E10 Ω
Low Resistance State	1mA Write Compliance Current	2.58E2 Ω	3.04E2 Ω	3.44E2 Ω	2.67E1 Ω
High Resistance State	1mA Write Compliance Current	2.02E4 Ω	9.08E4 Ω	2.97E5 Ω	7.89E4 Ω

W (Tungsten) Raw Die

Characteristic	Condition	Min	Type	Max	Std
Forward Adaptation Threshold	DC / quasi-static	0.150 V	0.258 V	0.350 V	0.049 V
Reverse Adaptation Threshold	DC / quasi-static	–0.270 V	–0.108 V	–0.050 V	0.057 V
Cycle Endurance	1.5 Vpp, 500 Hz sine wave, 50 kΩ Series resistor	50M	100M	5B	
Low Resistance State	100nA Write Compliance Current	1.04E6 Ω	1.38E6 Ω	2.16E6 Ω	3.01E5 Ω
High Resistance State	100nA Write Compliance Current	4.01E6 Ω	8.17E6 Ω	1.72E7 Ω	3.77E6 Ω
Low Resistance State	1uA Write Compliance Current	1.50E5 Ω	4.67E5 Ω	1.30E6 Ω	3.09E5 Ω
High Resistance State	1uA Write Compliance Current	5.39E6 Ω	1.40E7 Ω	5.40E7 Ω	1.40E7 Ω
Low Resistance State	10uA Write Compliance Current	2.66E4 Ω	6.74E4 Ω	1.72E5 Ω	4.62E4 Ω
High Resistance State	10uA Write Compliance Current	2.36E6 Ω	9.19E6 Ω	2.04E7 Ω	5.70E6 Ω

Low Resistance State	100uA Write Compliance Current	1.93 E3 Ω	7.86 E3 Ω	4.63 E4 Ω	1.30 E4 Ω
High Resistance State	100uA Write Compliance Current	1.99 E5 Ω	2.71 E6 Ω	1.60 E7 Ω	4.70 E6 Ω
Low Resistance State	1mA Write Compliance Current	2.65 E2 Ω	2.94 E2 Ω	3.53 E2 Ω	2.44 E1 Ω
High Resistance State	1mA Write Compliance Current	1.50 E4 Ω	5.60 E4 Ω	1.13 E5 Ω	2.84 E4 Ω

A.3 AC Response of the Raw Die Devices:

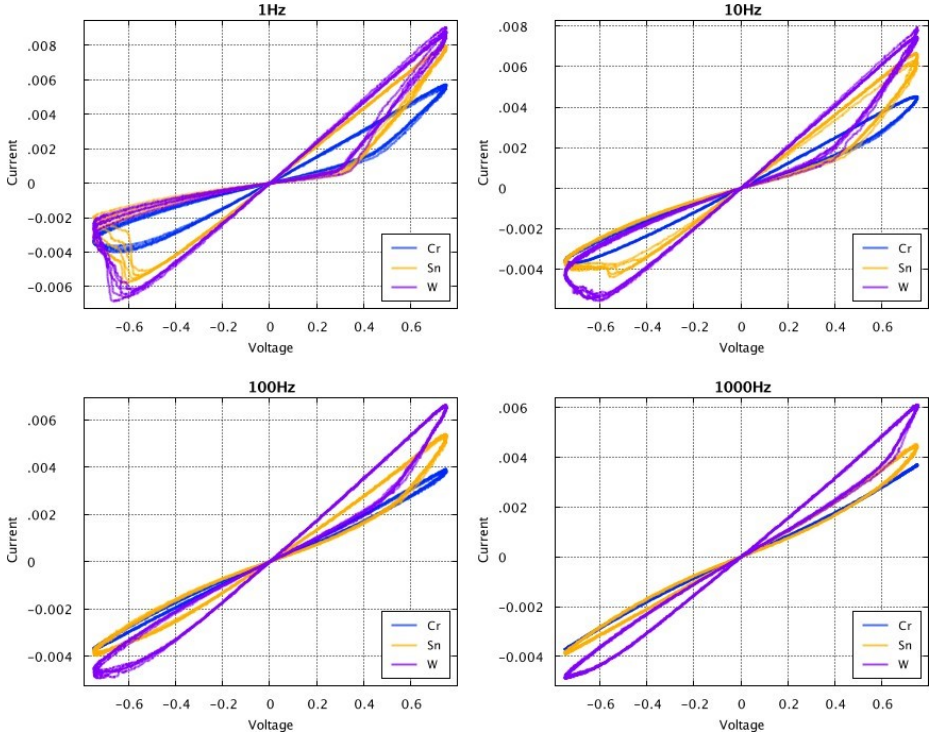

Memristor I-V CW Responses

A.4 CMOS+Memristor BEOL Service:

Via Known's collaboration with Boise State University, we offer the world's first CMOS Back End of Line (BEOL) Memristor service. We are offering this service to lower the barriers to memristive technology and help jump-start the memristor-based computing era. Multiple memristor types are possible covering a range of threshold voltages, resistance ranges, switching speeds, data retention, and cycling durability. Services includes layout design, all microfabrication steps for device fabrication, BEOL processing on CMOS die or wafers, wire bonding and packaging. Device electrical characterization possible over a frequency range of DC – 40 GHz, a temperature range of 4.2 K to 400 K, an optical excitation range of 190 nm to 1000 nm, and applied magnetic field from 0 to 5000 G.

BEOL Process

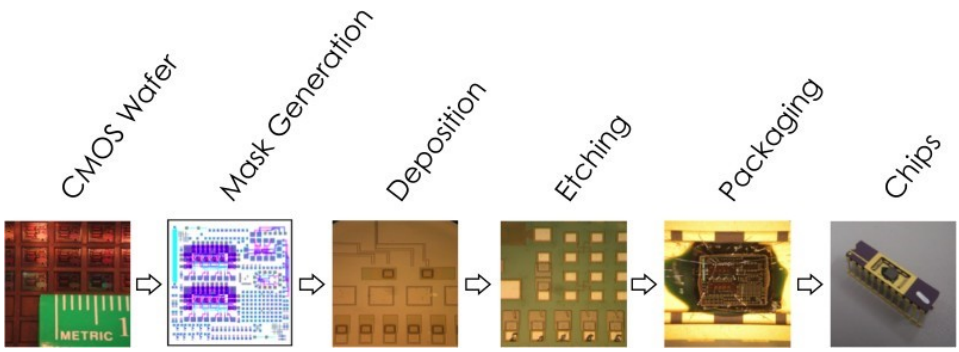

A.5 MSS Model:

Many memristive materials have recently been reported, and the trend continues. Memristor models are also being developed and incrementally improved upon. Our generalized metastable switch (MSS) memristor model is an accurate model that captures the behavior of memristors at a

level of abstraction sufficient to enable efficient circuit simulations while simultaneously describing a wide a range of possible devices. An MSS is an idealized two-state element that switches probabilistically between its two states as a function of applied voltage bias and temperature. A memristor is modeled by a collection of MSSs evolving in time, which captures the memory-enabling hysteresis behavior. In our semi-empirical model, the total current through the device comes from both a memory-dependent (MSS) current component, Im, and a Schottky diode current, Is in parallel:

$$I = \phi I_m (V, t) + (1 - \phi) Is (V)$$

, where $\phi \in [0, 1]$. A value of $\phi = 1$ represents a device that contains no Schottky diode effects. The Schottky diode effect accounts for the exponential behavior found in many devices and allows for the accurate modeling of that effect, which the MSS component cannot capture alone. The MSS model can be made more complex to account for failure modes, for example by making the MSS state potentials temporally variable. Multiple MSS models with different state potentials can be combined in parallel or series to model increasingly more complex state systems.

Appendix B

Analog Discovery 2 [51]

B.1 Overview:

The Digilent Analog Discovery 2™, developed in conjunction with Analog Devices, is a multi-function instrument that allows users to measure, visualize, generate, record, and control mixed signal circuits of all kinds. The low-cost Analog Discovery 2 is small enough to fit in your pocket, but powerful enough to replace a stack of lab equipment, providing engineering students, hobbyists, and electronics enthusiasts the freedom to work with analog and digital circuits in virtually any environment, in or out of the lab. The analog and digital inputs and outputs can be connected to a circuit using simple wire probes; alternatively, the Analog Discovery BNC Adapter and BNC probes can be used to connect and utilize the inputs and outputs. Driven by the free Waveforms software, the Analog Discovery 2 can be configured to work as any one of several traditional instruments, which include:

• Two-channel oscilloscope (1MΩ, ±25V, differential, 14- bit, 100Msample/sec, 30MHz+ bandwidth - with the Analog Discovery BNC Adapter Board).

• Two-channel arbitrary function generator (±5V, 14-bit, 100Msample/sec, 20MHz+ bandwidth - with the Analog Discovery BNC Adapter Board).

• Stereo audio amplifier to drive external headphones or speakers with replicated AWG signals.

• 16-channel pattern generator (3.3V CMOS, 100Msample/sec).

• 16-channel virtual digital I/O including buttons, switches, and LEDs – perfect for logic training applications.

• 16-channel digital logic analyzer (3.3V CMOS, 100Msample/sec).

• Two input/output digital trigger signals for linking multiple instruments (3.3V CMOS).

• Two programmable power supplies (0…+5V, 0…-5V. The maximum available output current and power depend on the Analog Discovery 2 powering choice.

• 250mW max for each supply or 500mW total when powered through USB.

• 700mA max or 2.1W max for each supply when using an external wall power supply.

• Single channel voltmeter (AC, DC, ±25V).

• Network analyzer – Bode, Nyquist, Nichols transfer diagrams of a circuit. Range: 1Hz to 10MHz.

• Spectrum Analyzer – power spectrum and spectral measurements (noise floor, SFDR, SNR, THD, etc.).

• Digital Bus Analyzers (SPI, I^2C, UART, Parallel).

The Analog Discovery 2

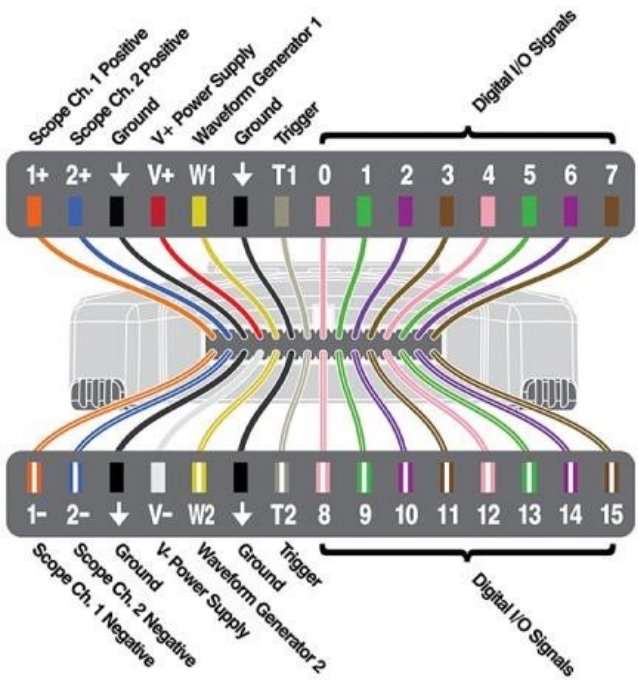

Analog Discovery 2 pinout diagram

B.2 Waveforms main window:

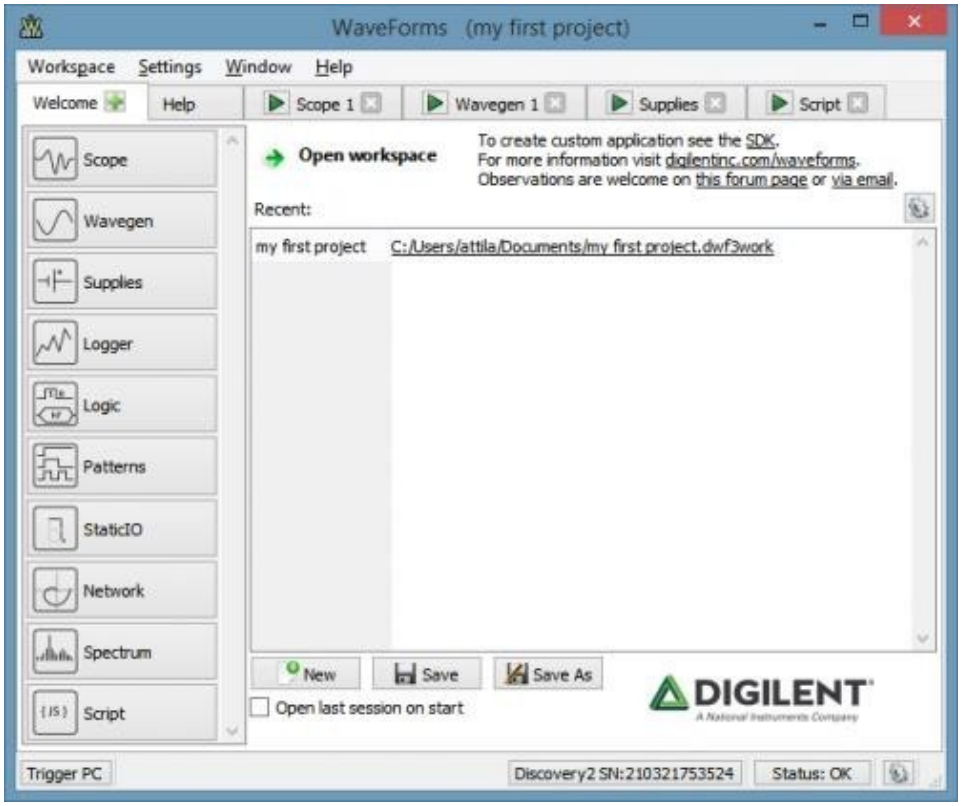

Waveforms main window.

B.3 Oscilloscope:

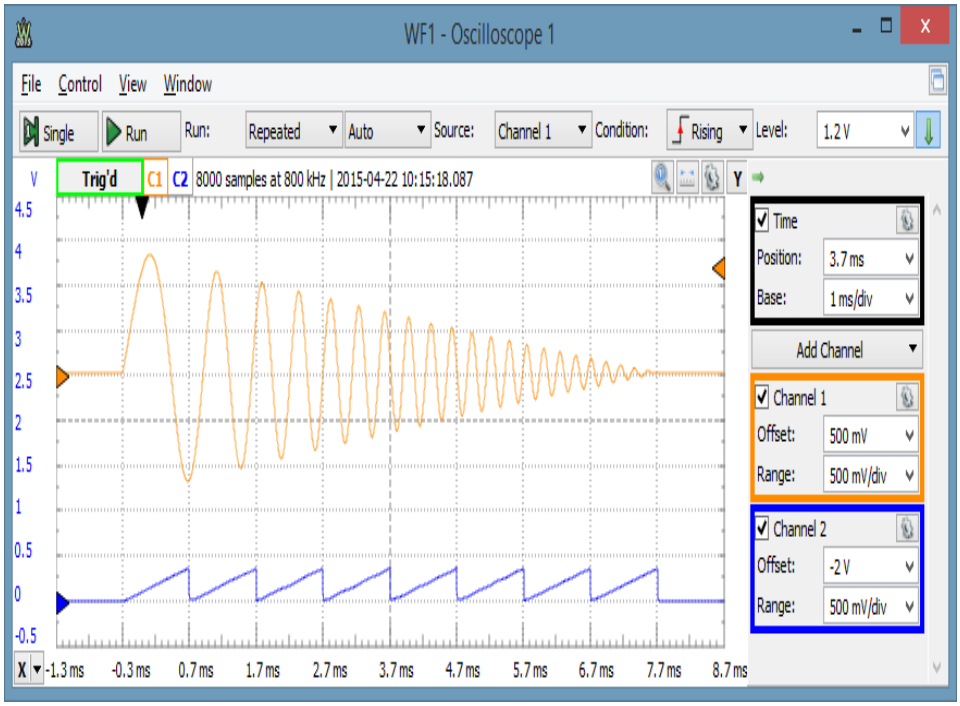

Oscilloscope graph.

B.4 Experimental Results with Digilent Analog Discovery:

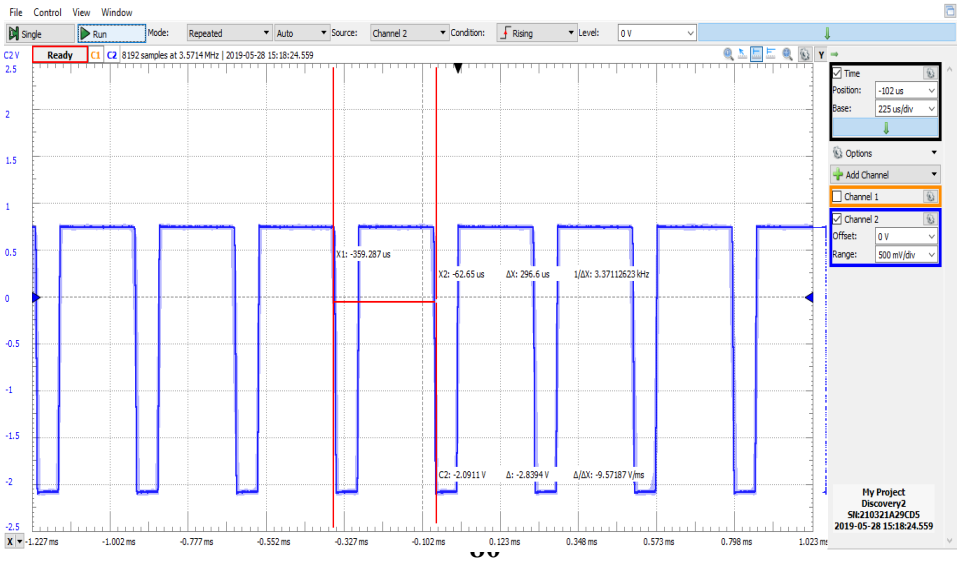

B.5 Experimental Results with Oscilloscope:

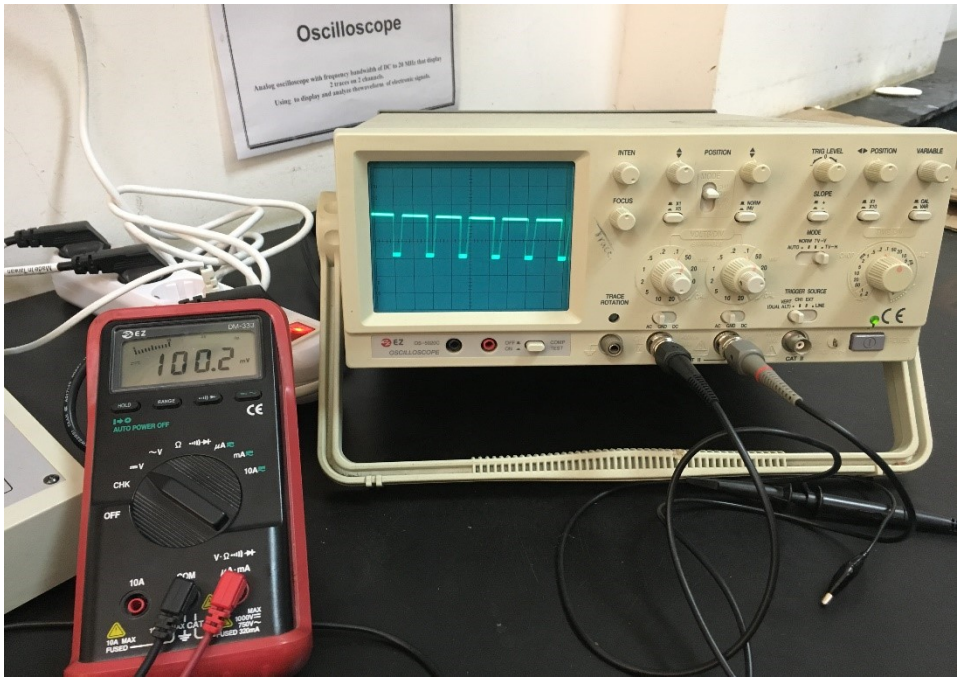

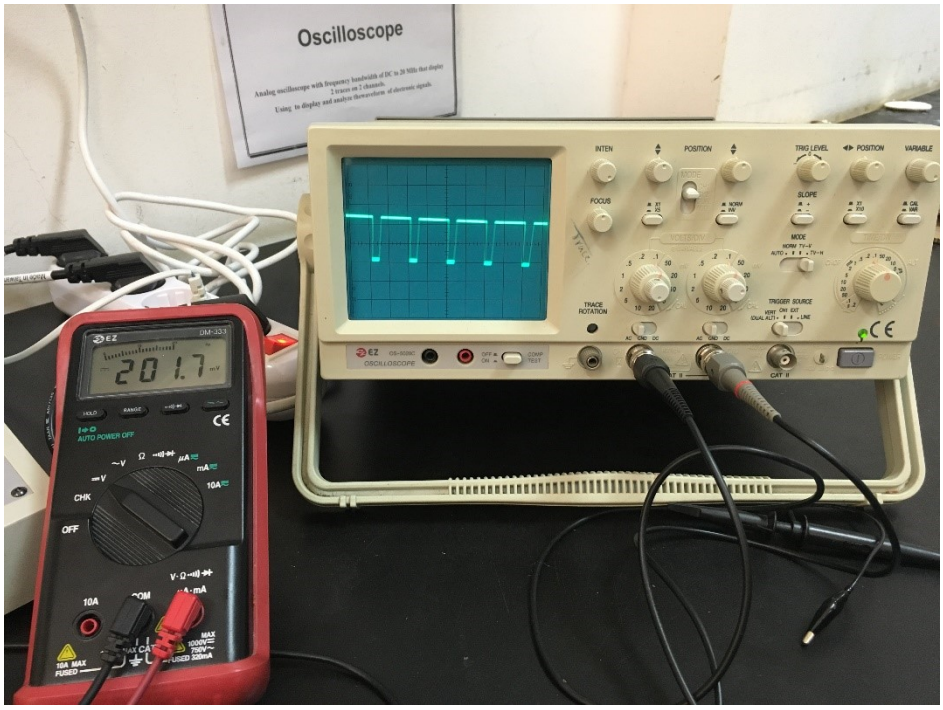
Oscilloscope
Analog oscilloscope with frequency bandwidth of DC to 20 MHz that display 2 traces on 2 channels
Using to display and analyze theswaveform of electronic signals
INTEN
POSITION
TRIG LEVEL
POSITION
VARIABLE
FOCUS
SLOPE
MODE
TRACE ROTATION
TRIGGER SOURCE
OSCILLOSCOPE
DM-333
201.7
AUTO POWER OFF
CHK
OFF
10A
10A MAX FUSED

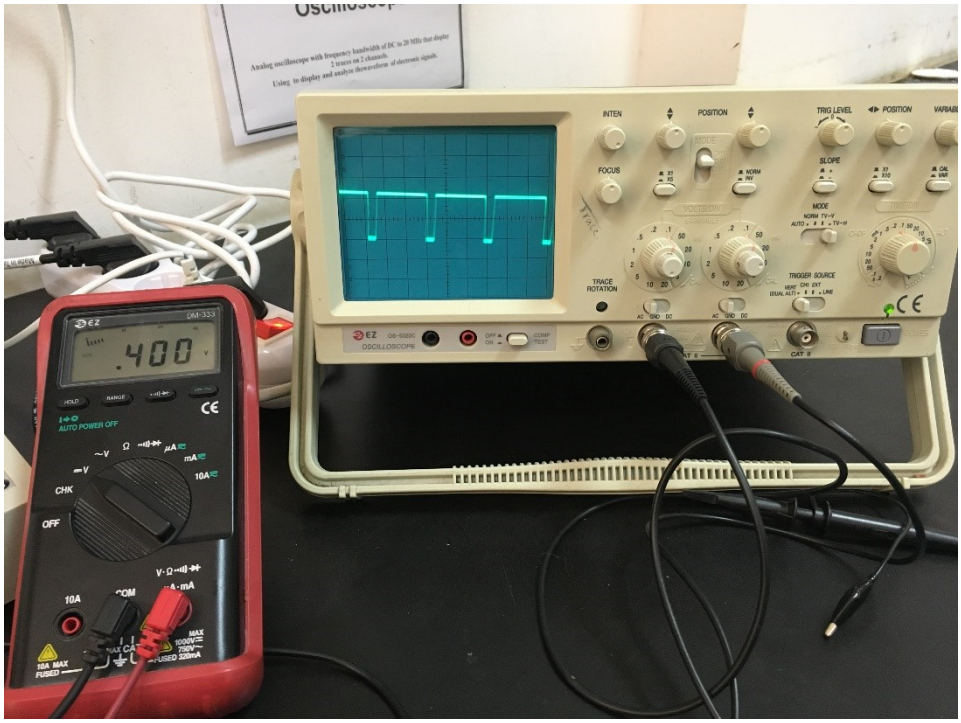
Analog oscilloscope with frequency bandwidth of DC to 20 MHz that display 2 traces on 2 channels
Using to display and analyze theswaveform of electronic signals
INTEN
POSITION
TRIG LEVEL
FOCUS
SLOPE
MODE
TRACE ROTATION
TRIGGER SOURCE
OSCILLOSCOPE
DM-333
.400
AUTO POWER OFF
CHK
OFF
10A
10A MAX FUSED